Articles in PresS. Am J Physiol Cell Physiol (September 20, 2017). doi:10.1152/ajpcell.00023.2017

Modulators of actin-myosin dissociation: basis for muscle type functional differences during fatigue

100 characters incl. spaces

Authors: Christina Karatzaferi [1,2], Nancy Adamek [3], and Michael A. Geeves [3]

[1] Muscle Physiology and Mechanics Group, DPESS, University of Thessaly, Karyes, Trikala, 42100, Greece

[2] Experimental Myology and Integrative Physiology Cluster, FSHS, University of St Mark and St John, UK

[3]School of Biosciences, University of Kent, Canterbury, CT2 7NH Kent, UK

Running head: Muscle type actomyosin dissociation differences in fatigue

58 characters incl. spaces

Address for correspondence: M.A. Geeves, School of Biological Sciences, University of Kent, Canterbury, CT2 7NH Kent, UK, M.A.Geeves@kent.ac.uk

Author contributions: CK & MAG conceived the study, MAG & CK designed the study, NA & CK collected data, NA created figures and tables, all co-wrote and edited the original manuscript, CK and MAG revised the manuscript.

Abstract

The muscle types present with variable fatigue tolerance, in part due to the myosin isoform expressed. However, the critical steps that define 'fatigability' *in vivo* of fast vs slow myosin isoforms, at the molecular level, are not yet fully understood. We examined the modulation of the ATP-induced myosin sub-fragment 1 (S1) dissociation from pyrene-actin by inorganic phosphate (Pi), pH and temperature using a specially modified stopped-flow system that allowed fast kinetics measurements at physiological temperature. We contrasted the properties of rabbit psoas (fast) and bovine masseter (slow) myosins (obtained from samples collected from New Zealand rabbits and from a licensed abattoir, respectively, according to institutional and national ethics permits). To identify ATP cycling biochemical intermediates, we assessed ATP binding to a pre-equilibrated mixture of actomyosin and variable [ADP], pH (pH 7 vs pH 6.2) and Pi (zero, 15 or 30 added mM Pi) in a range of temperatures (5 to 45^{o}C). Temperature and pH variations had little, if any, effect on the ADP dissociation constant (K_{ADP}) for fast S1 but for slow S1 K_{ADP} was weakened with increasing temperature or low pH. In the absence of ADP, the dissociation constant for phosphate (K_{Pi}) was weakened with increasing temperature for fast S1. In the presence of ADP, myosin type differences were revealed at the apparent phosphate affinity, depending on pH and temperature. Overall, the newly revealed kinetic differences between myosin types could help explain the *in vivo* observed muscle type functional differences at rest and during fatigue.

246 words

Keywords: myosin kinetics, cross-bridge cycle, temperature, muscle fatigue

Introduction

Myosin II exists in multiple isoforms (49) with *slow* muscles expressing the type 1 (MyHC-1 also known as β myosin) and *fast* muscles expressing one or more of the type 2 myosins (MyHC-2a, 2b, or 2x). Contraction depends directly on the interaction of myosin II multi-headed filaments, with filamentous 'tracks' of actin, arranged within the sarcomeres, the 'functional units' of muscle (28, 47). Eventually, whole muscle force output depends on the number of myosin cross-bridges interacting 'strongly' or 'weakly' with actin, while the velocity of contraction depends on the rate at which myosin detaches from actin at the end of the working stroke (11).

The study of kinetics of the actomyosin (A.M) interaction cycle identifies clear intermediate steps (for a review see (5)). Such studies have revealed that slow skeletal myosin heavy chain isoforms (MyHC 1) have distinct properties from fast isoforms (MyHC 2s), e.g. regarding ATPase activity and the rate and equilibrium constants of the various biochemical steps, which are expected to dictate their different mechanical properties. Thus, efficiency of actin-induced ADP displacement from myosin (the ratio of the ADP dissociation constant for A.M (K_{ADP}) over the ADP dissociation constant for myosin (K_D)), and strain sensitivity (dependence on external mechanical load) can differ substantially between fast and slow myosins (5, 22) , with slow myosins binding ADP tightly and releasing it at a slower rate than fast myosins. Consequently, ADP release is considered the rate limiting step for the maximum contraction velocity of slow muscles (29, 44), at least at the temperatures where fibers or myosin solutions are usually studied (10 to 22 °C).

The coupling of biochemical steps with mechanical events has, however, not been fully elucidated (22) while the 'laws' governing how ensembles of myosins integrate within the organized sarcomere (18, 19, 40) are not yet fully defined; this can be attributed partly to lack of physiologically relevant experimental evidence at the molecular level. This is especially true on the question of muscle fatigue, a complex multifaceted phenomenon.

At the organismal level, fatigue has a large heterogeneity of research outcomes (6) depending on the type, duration and intensity of muscular activity employed (8, 10), the muscle composition studied (24) and health status (30), etc. In terms of intramuscular biochemical changes, the degree of acidosis observed depends on the rate and extent to which anaerobic glycolysis is relied upon; which in turn is dependent on the fiber type and type of activity (i.e. more in 'supramaximal'/sprint type work, more in ischemia) as well as the presence and activity of lactate and proton transporters (see e.g. (32)). Brief very intense voluntary exercise has been shown, in mixed muscle, to lower pH from 7.1 to 6.4 (7, 8, 27, 31, 48) and to disturb the ATP and phosphocreatine levels, notably in fast, type II, fibers to near depletion (34, 35). Based on NMR data, ADP levels are calculated to rise to 200 μM (21) as, in healthy muscle, they are well buffered by the adenylate kinase and AMP deaminase reactions (26). Still, small variations in [ADP] can significantly affect the sarcoplasmic reticulum's function (39), and may help in maintaining tension economy (37). The drop in pH affects not only calcium sensitivity (20) but also the effect of accumulated Pi, which can reach 20-30mM in exercising muscle (2, 38), with its di-protonated form considered to inhibit force (for a review see (2)). At the myofibrillar level, changes in muscle mechanics during fatigue could be related to either reduction of energy substrates (e.g. causing localized ATP minima (34, 35)) and /or accumulation of ATP hydrolysis by-products (e.g. (14, 33, 37, 45, 53)). This is because the interaction of myosin with actin (actomyosin) is a multi-substrate and multistep reaction i.e. not only fueled by ATP hydrolysis but also modulated by ATP hydrolysis by-products (ADP, Pi, H^+) and other prevailing intracellular conditions (12). Thus, for the purposes of this work, fatigue is considered in the context of factors influencing the actomyosin cycle in a way to cause slowing of the cycle and/or weaker actomyosin interactions.

Overall, investigations ranging from whole body exercise (8, 30), to intact small muscles or fibers (59) to skinned fibers, (13, 14, 17, 33, 37, 46) or myofibrils (53), and few isolated molecule approaches [e.g. (16)] have provided strong evidence that the accumulation of inorganic phosphate (Pi) and of hydrogen ions can contribute to, if not cause, peripheral muscle fatigue. Still, their exact impact, especially at

104 physiological *in vivo* conditions, has attracted much debate (e.g. (58)). This is further
105 complicated by muscle type differences (fast vs slow) in energetics, myosin ATPase,
106 and mechanical performance (9, 49, 50) , which can be linked to a great degree to
107 inherent properties of the myosin II isoform expressed.

108 Our understanding of fatigue effects is further complicated by muscle type
109 differences (fast vs slow) in energetics, myosin ATPase, and mechanical performance
110 (9, 49, 50) , which can be linked to a great degree to inherent properties of the
111 myosin II isoform expressed. The steps that control the detachment of the myosin
112 cross-bridge at the end of the working stroke from actin are rapid and are thought to
113 limit the shortening velocity, a key parameter of muscle function. Temperature
114 predictions from kinetic studies of actomyosin in solution (44), suggest that the rate
115 of ADP release may limit unloaded velocity for both fast and slow myosin isoforms. It
116 can be hypothesized that such an ADP effect could be aggravated by the presence of
117 hydrogen ions and inorganic phosphate, as in fatigue, but it is not known if this is the
118 case and what would be the role of the myosin type.

119 Moreover, a parameter not often considered is temperature. *In vivo* mammalian
120 muscle temperature ranges from 32 to > 40 °C, while in severe fatigue, pH drops and
121 inorganic phosphate (Pi) accumulates (23) concomitantly. A number of *in vitro* fiber
122 studies at higher temperatures, have challenged long held views about the individual
123 role of the key 'fatigue' metabolites on mechanics, [e.g. less of an effect of pH (36,
124 45, 59)) or Pi on force, (13, 14, 17, 33)). Thus, it appears that employing
125 temperature modulations in the *in vitro* experimentation is necessary to tease out
126 physiological synergies [e.g. a synergism of myosin light chain phosphorylation with
127 low pH and high [Pi] became evident only at a high temperature (36)], if one wants
128 to realistically link muscle function *in vivo* to actomyosin interaction molecular
129 events studied *in vitro*. This necessitates molecular experimentation that mimics
130 physiology to the degree possible.

131 Therefore the purpose of this research was to study the fast kinetics of ATP-induced
132 dissociation of A.M. with and without ADP using the stopped flow. We examined the
133 interplay of 'fatigue' factors, e.g. low pH and high inorganic phosphate (Pi), with

myosin type, on ATP-induced dissociation of A.M. Taking advantage of recent methodological advancements we studied, for the first time, the ATP-induced dissociation of fast and slow S1 from actin in temperatures ranging from 5 to 45 ^{o}C to reveal critical myosin type and/or temperature dependencies of these processes.

Glossary & abbreviations

A.M: actomyosin complex
S1: myosin subfragment 1
actin.S1: actin bound with S1
K_1 : equilibrium constant for the formation of the complex of AM with ATP (denoted as A.M.T),
k_{+2}: rate constant of isomerization of A.M.T to A~M.T which is followed by actin dissociation
k_{obs}: observed rate constant of ATP induced dissociation of myosin from actin
K_{ADP}: dissociation constant for ADP
K_{Pi}: dissociation constant for phosphate
K_{ADP+Pi}: dissociation constant for ADP in the presence of phosphate
MyHC: myosin heavy chain

Materials and methods

Ethics Statement

Muscle tissue was obtained post-mortem from animals treated as recommended by national and local guidelines (UK Animals (Scientific Procedures) Act, 1986). Fast skeletal muscle came from the psoas muscle of New Zealand rabbits and slow skeletal muscle from bovine masseter.

Protein preparation

Myosin was prepared from the rabbit psoas (for fast MyHC-II) and the bovine masseter muscle (for slow MyHC-I) according to Margossian and Lowey (41) , and was subsequently digested to subfragment 1 (S1) with chymotrypsin as described by Weeds & Taylor (57) which removes the regulatory light chain region. These two muscle types yield essentially pure MyHC isoform (e.g. (1, 25) for rabbit psoas (isoform 2X) and (55) for bovine masseter (isoform 1) a result confirmed in routine

SDS-PAGE by us and others and by the expected value of K_{ADP} which is characteristic of a pure MyHC isoform (as indicated e.g. in (4)).

Actin was prepared from rabbit muscle as described by Spudich & Watt (52) and labelled with pyrene iodoacetamide to give pyrene-labelled actin as described by Criddle et al (15). Protein stocks of S1 and of pyrene-labelled actin were stored at 4^{o}C and were used for up to 2 weeks. In the text herein reference to actin implies pyrene-labelled actin.

Experimental buffers

The main buffer contained 20 mM cacodylate (adjusted at pH 7.0 or pH 6.2), 100 mM KCl, 5 mM $MgCl_2$ and 1 mM NaN_3; when phosphate was present in the buffer the ionic strength was adjusted accordingly to a final ionic strength of 170 mM. Concentrations (whether of proteins or buffer constituents) given in the text and figure legends refer to the concentration after mixing 1:1 in the stopped flow (unless stated otherwise).

Experimental equipment, procedures and analysis

Stopped-flow experiments were performed essentially as described previously (4) using a HiTech Scientific SF-61DX2 stopped flow system and 4-5 transients were acquired for each ATP transients (Kinetic Studio suite). The dead time of the equipment was 0.002 s. A wide temperature range (5 – 45 ^{o}C) for measurements was available because of a new adaptation of the standard stopped flow machine (see (56)). Briefly, the drive syringes were held at room temperature (20 °C) while loading lines leading into the mixing chamber, the mixing and observation chamber were all thermostated at the temperature of the measurement. Essentially the samples were only exposed to the temperature of the measurement for a few seconds, thus allowing measurements of proteins under conditions where they are not usually stable for long.

The **ATP induced dissociation rate of actin.S1**, was measured in the stopped-flow by mixing a fixed concentration of pyr.actin.S1 complex (end concentration 0.25 μM) with excess ATP and monitoring fluorescence transients from the pyrene-labeled

actin (excitation at 365 nm, emission through a KV389 nm cut-off filter (Schott, Mainz, Germany)). Details of the kinetic analysis are given under data fitting.

In a similar process, **ADP dissociation constant** (K_{ADP}), which defines ADP affinity for actin.S1, was measured by adding to the mixture ADP as a competitive inhibitor of ATP binding. In this case it is convenient to add the ADP to the ATP solution, i.e. 0.5 µM pyr.actin.S1 was mixed with 25 µM ATP with various concentrations of ADP present with the ATP (from 0 to 1200 µM). This approach assumes that ADP is in rapid equilibrium with the actin.S1 complex on the time scale of the ATP induced dissociation reaction. This was ensured by using the low (25 µM) concentration of ATP. That this assumption holds was tested by repeating the measurement with ADP pre-incubated with actin.S1 and then mixing with ATP. The observed rate constants were identical in each case. Details of the data analysis are given below (see Scheme 1 on the competitive inhibitor approach, and equation 4).

Phosphate dissociation constant (K_{Pi}) was measured exactly as for the ADP dissociation constant except that the high concentrations of Pi used meant it was more convenient to have P_i present in the buffer in both syringes of the stopped-flow. Details of the data analysis are given below (see Scheme 1 on the competitive inhibitor approach, and equations 5 and 6).

ADP dissociation constant in the presence of phosphate (K_{ADP+Pi}) was also measured using the same approach as for K_{ADP} but using buffers containing fixed amounts of inorganic phosphate, 30 mM in the case of psoas S1 and 15 mM with masseter S1. The different affinities of Pi for the two types of S1 required a different concentration of Pi. Preliminary data indicated that Pi binding to psoas S1 was > 10 mM and weaker than to masseter S1, by approximately a factor of 2. Since the limits of ionic strength precluded using saturation amounts of Pi we used a Pi concentration close to the range of K_{Pi} values.

Experiments were performed at two pH levels, 7 and 6.2 and in a range of temperatures. Care was taken to reverse the order of experiments to avoid the

possibility of a time and 'order' effect either with respects to pH or temperature.

Data Fitting and Interpretation Approach

In the present study we focused our attention on the ATP induced dissociation of actin.S1. This is the step that controls the detachment of the actomyosin cross-bridge at the end of the working stroke.

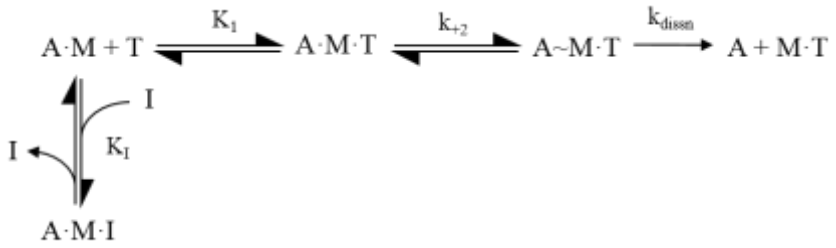

Scheme 1. Model of ATP-induced dissociation of actin.S1 based on Millar and Geeves (42) .

In Scheme 1, T = ATP; A = actin; M = myosin; I is an inhibitor, competitive with ATP for the nucleotide binding site. K_1 defines the equilibrium constant for the formation of the A.M.T collision complex, which is followed by an almost irreversible isomerization of the complex to the ternary complex A~M.T with the rate constant of k_{+2}. This is rapidly followed by dissociation of actin from the ternary complex. K_I is defined as a dissociation constant k_{-I}/k_{+I}. In the experiments presented here the inhibitor was either ADP or inorganic phosphate (P_i).

The reaction described in Scheme 1 was monitored through pyrene fluorescence changes which monitor the ATP induced dissociation of actin from the complex (fluorescence increases by up to 70 %.), specifically associated with step 2 of Scheme 1, (see in Results, Fig. 1A). Four to five transients were collected for each ATP concentration used then averaged before further analysis.

The averaged transients were fitted with single (eqn1) or, if needed, a double exponential equation (eqn2):

$$F_t = \Delta F \cdot e^{(-k_{obs} \cdot t)} + F_\infty \qquad \textit{eqn 1}$$

or

$$F_t = \Delta F_{(1)} \cdot e^{(-k_{obs(1)} \cdot t)} + \Delta F_{(2)} \cdot e^{(-k_{obs(2)} \cdot t)} + F_\infty \qquad \textit{eqn 2}$$

Where F_t is the observed fluorescence at time t, F_∞ is the fluorescence at the end of the transient (t= ∞) and ΔF is the total change of fluorescence observed. The observed rate constant (k_{obs}) reflects the ATP induced dissociation rate of actin.S1 and is linearly dependent on [ATP], at the ATP concentrations used here. A plot of [ATP] vs k_{obs} was used to derive the values of K_1 and k_{+2} (using Origin v 6.0), as defined in scheme 1 and eqn 3.

$$k_{obs} = K_1 k_{+2}[ATP] \qquad \textit{eqn 3}$$

The presence of a competitive inhibitor to ATP binding (that does not induce actin.S1 dissociation) would appear to slow the rate of actin.S1 dissociation. If inhibitor binding is in rapid equilibrium with actin.S1, within the timescale of data acquisition, compared to the rate of ATP-induced dissociation of actin.S1 (i.e. $k_{+AD} + [ADP]k_{-AD} >> K_1 k_{+2}[ATP]$) , then

$$k_{obs} = K_1 k_{+2}[ATP]/(1 + ([I]/K_I)) \qquad \textit{eqn 4}$$

Then, plotting k_{obs} as a function of [I] will allow the K_I (in scheme 1) to be defined. This approach was used to define the value of K_I for ADP (K_{ADP}) and Pi (K_{Pi}).

If both ADP and Pi are present in the same measurement, two scenarios are possible. If both compete for the same binding site then the effect of the two inhibitors is additive and the effect on k_{obs} can be predicted from the values of K_{ADP} and K_{Pi} measured independently.

$$k_{obs} = K_1 k_{+2}[ATP]/(1 + ([ADP]/K_{ADP}) + ([Pi]/K_{Pi})) \quad \text{eqn 5}$$

where the measured K_I with variation of [ADP] and fixed [Pi] is $K_I = 1/K_{ADP} + [Pi]/K_{Pi}$

If both however bind into the ATP pocket at the same time to create the complex A.M.ADP.Pi then the above relationship will not hold and Pi will alter the affinity of A.M for ADP.

The apparent affinity of ADP for actin.S1 (K_{ADP+Pi}) was measured for several concentrations of Pi and then the dissociation constant of Pi calculated according to the following relationship and compared with the value of $K_{PI.}$

$$K_{Pi\ app} = [Pi]/(K_{ADP+Pi}/K_{ADP} – 1) \qquad \text{eqn 6}$$

ADP release rate constant. Two types of myosins were studied which are known to differ in their dissociation constant for nucleotides (5, 51). The rate constant for the release of ADP (k_{-ADP}) is relatively slow for masseter S1 and can easily be measured in an ADP displacement experiment. This step is very fast for a fast muscle isoform and too fast to measure by current equipment. Briefly, actin.^{Mass}S1 saturated with 75 µM of ADP (A.M.D complex) was mixed with a large excess of ATP (8 mM) in the stopped-flow. Then the k_{obs} values, fitted to a single exponential equation (eqn 1) defined the rate constant by which ADP is released by the ternary A.M.D complex (k_{-AD}).

The data presented in the figures are the values for the individual experiment displayed, while the data values presented in the table 1 are averaged values for n = independent day measurements.

The *temperature dependence* of the above studied biochemical steps K_1k_{+2}, K_{ADP}, K_{Pi} and K_{ADP+Pi} data were plotted as the natural logarithm of the measured parameter against the reciprocal of temperature in degrees Kelvin (1/T ^{o}K) and fitted with linear regression using the Arrhenius (rate constants) or Van't Hoff (equilibrium constants) equations

$$\ln K_1k_{+2} = \ln (A) - Ea/RT \qquad \text{eqn 7}$$

$$\text{Ln Keq} = \Delta S°/R - \Delta H°/RT \qquad \text{eqn 8}$$

where Ea stands for activation energy, R is the gas constant, A is a pre-exponential factor. The values of –Ea/R or or $\Delta H°/R$ were derived from the slopes.

Results & Discussion

ATP induced dissociation rate of actin.S1. When actin.^{Pso}S1 and actin.^{Mass}S1 were mixed with ATP, as shown in Figure 1 A and B, the observed stopped-flow transients were described by a single exponential for both myosin isoforms (Fig 1A and 1B). Keeping a fixed ATP concentration and increasing the temperature allows the best estimate of the temperature dependence of the reaction since it minimizes variation in ATP concentration between experiments. Increasing the temperature from 5-43 °C reduced the total fluorescence signal by ~ 40% due to collisional quenching but the signal change remained relatively constant with an approximately 2-fold increase in fluorescence observed in all transients. The transients were therefore normalized to illustrate the change in the k_{obs} values. For *psoas* (Fig 1 A) and *masseter* (Fig 1 B) temperature increased the k_{obs} value ~3 fold in both cases over the range of measurements from 3 to 43 °C. The figure shows illustrative examples of one set of transients.

Lowering the pH to 6.2 slightly increased the k_{obs} values for both isoforms by about 20-25 % (and hence the second order rate constant $K_1k_{+2,}$ see Table 1). Increasing temperature resulted in an average increase of 3 fold over the temperature range of 5-35 °C. The amplitudes of the transients at pH 6.2 were again relatively stable and similar to pH 7 for ^{Pso}S1 at 43 %. For ^{Mass}S1 the amplitudes were also stable in pH 6.2 but showed an overall increase in fluorescence from 40 to 50% of total fluorescence signal.

Effect of temperature: The temperature dependence of the dissociation rate constant was examined at pH 7 and then repeated at pH 6.2 (Fig 1C and 1D). Each measurement was repeated 3 times and the average values collated in Table 2. The Arrhenius plots of the temperature dependence measurements at pH 7 and 6.2 gave well defined straight lines over the temperature range (5 – 43 ^{o}C). In the absence of phosphate, for *psoas* the activation energy (Ea) values were very similar at pH 7.0 and 6.2 as shown in Figure 1 C, 28.3 ± 0.8 and 29.3 ± 0.8 kJ/mol respectively. For masseter, Ea values were on average lower than the ones for fast, being for pH 7.0 and 6.2, 25.7 ± 1.4 and 23.8 ± 1.1 kJ/mol respectively (Figure 1D).

Effect of Pi and pH: When the ATP-induced dissociation measurements were repeated in the presence of high phosphate concentrations, of the order that might be expected in fatigue, the observed rate constants for the dissociation reaction were 2-fold slower for ^{Mass}S1 and 2- to 3-fold slower for ^{Pso}S1 at both pH levels compared to the data in the absence of phosphate. This is consistent with Pi acting as a competitive inhibitor with a K_i of 10 – 20 mM. It should be noted that while 30 mM Pi was used for ^{Pso}S1, 15 mM Pi was used for ^{Mass}S1 experiments.

The transients of both isoforms had bi-phasic tendencies at the low temperatures (5-10 °C) at both pHs, but were single exponential at all other temperatures. The origin of this additional slow phase, which had a very small amplitude (1-3 %), is not known, but possible contamination by ADP was eliminated by control measurements in the presence of apyrase which converts any ADP present, which does not bind to S1, to AMP.

The amplitudes of the dissociation reaction were 50 % smaller/reduced in the presence of phosphate for both, ^{Pso}S1 and ^{Mass}S1, indicating some loss of affinity of S1 for actin in the presence of Pi. However, for psoas the amplitudes increased with temperature from 25 to 30 % at pH 7.0 and even more dramatically from 12 to 20 % at pH 6.2. This behavior was not observed with ^{Mass}S1 *masseter*.

Combined effect of temperature, pH and phosphate: the temperature dependence of the dissociation rate constant in the presence of phosphate is shown in Figure 2 and the activation energies determined for *psoas* (38 ± 1 kJ/mol) and *masseter* (30 ± 1 kJ/mol) were greater than in the absence of Pi, irrespective of the pH used. Thus phosphate increased the activation energy of ^{Pso}S1 at both pH values by about 10 kJ/mol, which is a larger increase than observed with *masseter*, where the increase was only about 5 kJ/mol in the presence of phosphate.

Rate constant of ADP release (k_{-ADP}) was evaluated by an ADP displacement experiment, mixing actin.^{Mass}S1 saturated with ADP with an excess of ATP. This measurement was not possible for ^{Psoas}S1 because the ADP release is too fast to measure.

Displacement of ADP from actin.^{Mass}S1 by a large excess of ATP was biphasic. The transients were well-defined with stable amplitudes of 24 and 6 % for the fast and slow phase, respectively (as shown in Figure 3 A). These amplitudes were similar under all conditions explored. The fast phase defines the rate constant at which ADP is released and is thought to limit the velocity of shortening of a masseter muscle (4). The slower phase is an off pathway event and will not be considered further here. The k_{obs} of the ADP release was 85 s^{-1} at 20 °C (pH 7.0) and compares well to published results of 94 s^{-1} by Bloemink et al (4).

The reaction was measured over the temperature range of 5 - 30 °C at pH 6.2 and 7.0, and in the presence of 15 mM Pi. The k_{obs} values are summarized in the Arrhenius plot in Fig 3B. The k_{obs} values increased from 16.2 at 5 °C to 273 s^{-1} at 30 °C with similar values at pH 7.0 and pH 6.2 throughout the temperature range used. Above 30 °C the reaction was too fast to measure reliably. Thus the activation energy was large with similar values at both pH levels studied.

The addition of 15 mM Pi had little effect at pH 7.0. At pH 6.2 however we saw a 30-50 % increase in k_{obs} in the presence of phosphate and a small change in the activation energy.

ADP dissociation constant (K_{ADP})

The ADP dissociation constant (K_{ADP}) for pyr.actin.S1 was measured by the competitive inhibitor approach as described in the Methods.

ADP included in the ATP solution competes with ATP for binding to the pyr.actin.S1 and slows the k_{obs} value as shown in Fig 4. The ADP dissociation constant was 168 µM for ^{Pso}S1 and 31 µM for ^{Mass}S1 at 20 °C and pH 7.0, as reported previously (22). This large difference in the affinity of actin.S1 for ADP is a major characteristic of a fast vs a slow myosin isoform. As reported previously the ADP affinity for *psoas* actin.S1 was relatively unaffected by temperature (about 200 ±30 µM between 10

and 30 °C) while for *masseter* the effect was much greater, with the affinity becoming weaker by ~6-fold from 9.6 µM at 10 °C to 62.4 at 30 °C, at pH 7.0.

Effect of pH: A change in pH did not affect the ADP affinity for *psoas* (Table 1) over the temperature range studied (also Figure 4C). Lowering the pH to 6.2 with ^{Mass}S1 resulted in 2-fold weaker K_{ADP} values than at pH 7.0 (from 10 to 22 µM at 10 °C). However, this effect of pH was not as pronounced at higher temperatures (only weakening by 1.5 fold at 30 °C, see Table 1).

Phosphate dissociation constant (K_{Pi})

The dissociation constant of Pi for actin.S1 (K_{Pi}) was measured but the range of Pi concentrations accessible was restricted by the need to maintain a constant ionic strength. As P_i was increased the concentration of KCl in the buffer was decreased and the maximum phosphate concentration used was 30 mM. Figure 6 shows the plots of k_{obs} as a function of phosphate concentration for the two myosin isoforms. These show the expected inhibition as [Pi] is increased with an average K_{Pi} value of 15 mM at 10 °C decreasing to 41 mM at 40 °C for actin.^{Pso}S1 at pH 7.0. Decreasing the pH to 6.2 did not significantly affect the K_{Pi} values for ^{Pso}S1 (11 mM at 10 °C, decreasing to 32 mM at 40 °C, see also Table 1).

Repeating the measurements with ^{Mass}S1 gave a K_{Pi} of 22 mM at 10 °C, weakened to 35 mM at 20 °C (pH 7.0). Lowering the pH to 6.2 resulted in an average K_{Pi} value of 17 mM at 10 °C, weakening to 28 mM at 40 °C. Thus a differential response of slow myosin to Pi was observed with temperature, with the slow myosin while starting off less sensitive to Pi at 10°C becoming more sensitive to Pi at 40°C.

ADP dissociation constant in the presence of phosphate (K_{ADP+Pi}) was evaluated as for the ADP dissociation constant but using fixed amounts of inorganic phosphate (30 mM in the case of ^{Pso}S1 and 15 mM with ^{Mass}S1). The presence of 30 mM Pi weakened the ADP dissociation constant (K_{ADP+Pi}) for actin.^{Pso}S1 3-4-fold (from about 170 µM to 890 µM at 20 °C (pH 7.0)) as shown in Figure 5A and Table 1. Repeating

the measurement at different temperatures showed the apparent K_{ADP} weakening from around 500 µM at 10-20 °C to 942 µM at 30 °C (Fig 5C and Table 1). For *masseter* the effects of Pi were less marked, with the K_{ADP} weakening only 1-2-fold across the temperature range at pH 7.0. Overall, it appears that phosphate competes with ADP binding to fast A.M, but has little effect on ADP binding in slow A.M. The formation of an A.M.ADP.Pi complex (see *Data Fitting and Interpretation Approach*) is not supported under our experimental conditions.

Lowering the pH to 6.2 resulted in a smaller effect of phosphate on the ADP dissociation constant for actin.^{Pso}S1, changing only 2-fold from 228 to 514 µM at 20 °C (compared to the 3 to 4-fold change seen at pH 7.0). This reduced effect of phosphate was seen across the temperature range used. In actin.^{Mass}S1, 15 mM Pi weakened the ADP affinity 2-fold from 47 to 94 µM at 20 °C, and a similar 2-fold weakening of the K_{ADP} in phosphate (K_{ADP+Pi}) was seen at the other temperatures used at pH 6.2.

Apparent phosphate dissociation constant ($K_{Pi\ app}$)

The apparent dissociation constant of phosphate for acto-myosinS1 ($K_{Pi\ app}$) in the presence of ADP was calculated from the ADP dissociation constants measured in the absence (K_{ADP}) and presence of phosphate (K_{ADP+Pi}) as detailed in the methods. At pH 7.0 and low temperature the $K_{Pi\ app}$ of actin.^{Pso}S1 was similar to the K_{Pi} value measured (11mM and 16 mM, respectively at 10 °C). At higher temperatures the K_{Pi} of actin.^{Pso}S1 was weakened to 30-40 mM, the $K_{Pi\ app}$ however remained at about 10 mM for the whole temperature range used.

At pH 6.2 the K_{Pi} of *psoas* was 30 % tighter than at pH 7.0 but otherwise showed the same behavior as temperature was increased (weakening from 15 mM at 10 °C to 32 mM at 40 °C). The $K_{Pi\ app}$ however appears 2-fold weaker at pH 6.2 for *psoas* with 24 mM and tightens to about 16 mM as temperature is increased.

For actin.^{Mass}S1 we observed a different behavior of the apparent phosphate dissociation constant; while the measured K_{Pi} values at pH 7.0 were similar to *psoas* across the temperature range used, the $K_{Pi\ app}$ showed distinct temperature dependence, weakening from 10 to 40 mM with temperature. The K_{Pi} values of

masseter were unaffected by a change in pH to 6.2 and remained similar to *psoas* at 22 and 35 mM (10 and 20 °C, respectively). The $K_{Pi\ app}$ however lost its temperature dependence when the pH was lowered to 6.2 and the value remained relatively unaffected at 10-15 mM for actin.^{Mass}S1 throughout the temperature range used.

Relevance to working muscle. Work by us and others indicated an important role for Pi in tension generation as conditions that affect actomyosin affinity, would affect, in proportion, force generation. With the assumption that A.M force-generating states are in an effective equilibrium with the non-force-generating states at the beginning of the working stroke, past skinned psoas fiber work suggested that, with increasing [Pi] the free energy of the states that precede Pi release decrease as −RT ln[Pi] (from the slope of the force-ln[Pi] relationship, relative to the free energy of states after Pi release, leading to progressive depopulation of the force-generating states and thus reducing tension generation (33). Earlier observations by Tesi et al (54) highlighted differences between slow and fast myofibrils in tension response to phosphate, with indications of stronger actomyosin bonds in slow muscle. The combination of low pH and high Pi was shown to synergistically inhibit velocity of contraction in skinned fibres (36, 43) adding further support to the notion that in fatigue conditions, the combined effect of Pi and protons on muscle performance would come about either by decreasing the force per bridge and/or increasing the number of low-force bridges. These and other studies indicated that the effect of Pi on its own is moderate at higher temperatures but in combination with low pH it can substantially affect muscle power by affecting actomyosin interaction. The present work adds important information to explain how Pi's interaction changes the ADP dissociation constant for AM and ultimately ATP-induced dissociation of AM, thus the speed of the cross-bridge cycle.

Concluding remarks

The phenomena we studied are at a lower level of component configuration, actin and myosin S1 in solution. We cannot therefore account for myosin cooperativity and coordinated responses to load, which could affect the hypothesized limiting processes. While experimental data imply such cooperativities (3) emerging

behaviors are difficult to assess and model, a situation further complicated by the difficulty of incorporating intra-head actions into models (40). At the macroscopic level, many studies have examined fatigue effects on mechanical function using single fibers (most however at non-physiological temperature); there are also isolated muscle and whole limb investigations (however with no control over metabolites levels); all these macroscopic studies have theorized about what may be occurring at the molecular level. Fewer studies have attempted a 'molecular explanation' of how velocity is affected in muscle fatigue (e.g. using in vitro motility (16)). Ours is the first study to employ solution transient kinetics to study how key fatigue factors affect the ATP-induced dissociation step of fast and slow S1 from actin (a critical part of the cycle that affects overall velocity). More information of the other events in the cycle, and the temperature dependence of these events for both fiber types, is needed to support future modelling attempts.

It remains to be seen how our findings can be integrated at the higher level 'behavior' of large myosin ensembles interacting with actin filaments, outside or inside an organized sarcomere. It is expected that in such situations other laws may apply when the myosin type effect on contractile behavior is further modulated depending on interactions with intracellular factors and overall muscle action regulation.

We expect that, given the undisputed phenotypic effect of myosin types as observed in mammalian physiology, our data provide highly relevant insights in the mechanochemical coupling factors that distinguish the fiber types. Phosphate dependence of ATP-induced dissociation is modulated by variations in actin affinity. Such variations could help modulate the phosphate dependence of force and velocity, and may explain why phosphate sensitivity appears to be in part temperature-and muscle type-dependent.

Acknowledgements

The authors acknowledge support from various sources as follows:

MAG was supported by the British Heart Foundation grant PG30200. Also, CK, MAG research was co-financed by the European Union (European Social Fund – ESF) and Greek national funds through the Operational Program "Educational and Lifelong Learning" of the National Strategic Reference Framework (NSRF) – Research Funding Program: Thales (MuscleFun Project-MIS 377260) Investing in knowledge society through the European Social Fund.

CK thanks COST Action CM1306 'Understanding Movement and Mechanism in Molecular Machines' for relevant networking support.

References

1. **Aigner S, Gohlsch B, Hamalainen N, Staron RS, Uber A, Wehrle U, and Pette D**. Fast myosin heavy chain diversity in skeletal muscles of the rabbit: heavy chain IId, not IIb predominates. *European journal of biochemistry* 211: 367-372, 1993.
2. **Allen DG, and Trajanovska S**. The multiple roles of phosphate in muscle fatigue. *Frontiers in physiology* 3: 463, 2012.
3. **Baker JE**. Muscle force emerges from dynamic actin-myosin networks, not from independent force generators. *American journal of physiology Cell physiology* 284: C1678; author reply C1678-1679, 2003.
4. **Bloemink MJ, Adamek N, Reggiani C, and Geeves MA**. Kinetic analysis of the slow skeletal myosin MHC-1 isoform from bovine masseter muscle. *Journal of molecular biology* 373: 1184-1197, 2007.
5. **Bloemink MJ, and Geeves MA**. Shaking the myosin family tree: biochemical kinetics defines four types of myosin motor. *Seminars in cell & developmental biology* 22: 961-967, 2011.
6. **Bogdanis GC**. Effects of physical activity and inactivity on muscle fatigue. *Frontiers in physiology* 3: 142, 2012.
7. **Bogdanis GC, Nevill ME, Boobis LH, Lakomy HK, and Nevill AM**. Recovery of power output and muscle metabolites following 30 s of maximal sprint cycling in man. *The Journal of physiology* 482 (Pt 2): 467-480, 1995.
8. **Bogdanis GC, Nevill ME, Lakomy HK, and Boobis LH**. Power output and muscle metabolism during and following recovery from 10 and 20 s of maximal sprint exercise in humans. *Acta physiologica Scandinavica* 163: 261-272, 1998.
9. **Bottinelli R**. Functional heterogeneity of mammalian single muscle fibres: do myosin isoforms tell the whole story? *Pflugers Archiv : European journal of physiology* 443: 6-17, 2001.
10. **Cannon DT, Howe FA, Whipp BJ, Ward SA, McIntyre DJ, Ladroue C, Griffiths JR, Kemp GJ, and Rossiter HB**. Muscle metabolism and activation heterogeneity by combined 31P chemical shift and T2 imaging, and pulmonary O2 uptake during incremental knee-extensor exercise. *Journal of applied physiology* 115: 839-849, 2013.
11. **Cooke R**. Force generation in muscle. *Current opinion in cell biology* 2: 62-66, 1990.
12. **Cooke R**. Modulation of the actomyosin interaction during fatigue of skeletal muscle. *Muscle & nerve* 36: 756-777, 2007.
13. **Cooke R, Franks K, Luciani GB, and Pate E**. The inhibition of rabbit skeletal muscle contraction by hydrogen ions and phosphate. *The Journal of physiology* 395: 77-97, 1988.
14. **Coupland ME, Puchert E, and Ranatunga KW**. Temperature dependence of active tension in mammalian (rabbit psoas) muscle fibres: effect of inorganic phosphate. *The Journal of physiology* 536: 879-891, 2001.
15. **Criddle AH, Geeves MA, and Jeffries T**. The use of actin labelled with N-(1-pyrenyl)iodoacetamide to study the interaction of actin with myosin subfragments and troponin/tropomyosin. *The Biochemical journal* 232: 343-349, 1985.
16. **Debold EP, Beck SE, and Warshaw DM**. Effect of low pH on single skeletal muscle myosin mechanics and kinetics. *American journal of physiology Cell physiology* 295: C173-179, 2008.
17. **Debold EP, Dave H, and Fitts RH**. Fiber type and temperature dependence of inorganic phosphate: implications for fatigue. *American journal of physiology Cell physiology* 287: C673-681, 2004.
18. **Debold EP, Walcott S, Woodward M, and Turner MA**. Direct observation of phosphate inhibiting the force-generating capacity of a miniensemble of Myosin molecules. *Biophysical journal* 105: 2374-2384, 2013.

19. **Egan P, Moore J, Schunn C, Cagan J, and LeDuc P**. Emergent Systems Energy Laws for Predicting Myosin Ensemble Processivity. *PLoS Computational Biology* 11: 2015.
20. **Fabiato A, and Fabiato F**. Effects of pH on the myofilaments and the sarcoplasmic reticulum of skinned cells from cardiace and skeletal muscles. *The Journal of physiology* 276: 233-255, 1978.
21. **Fitts RH**. Muscle fatigue: the cellular aspects. *Am J Sports Med* 24: S9-13.
22. **Geeves MA**. Review: The ATPase mechanism of myosin and actomyosin. *Biopolymers* 105: 483-491, 2016.
23. **Green HJ**. Mechanisms of muscle fatigue in intense exercise. *Journal of sports sciences* 15: 247-256, 1997.
24. **Hamada T, Sale DG, MacDougall JD, and Tarnopolsky MA**. Interaction of fibre type, potentiation and fatigue in human knee extensor muscles. *Acta physiologica Scandinavica* 178: 165-173, 2003.
25. **Hamalainen N, and Pette D**. The histochemical profiles of fast fiber types IIB, IID, and IIA in skeletal muscles of mouse, rat, and rabbit. *The journal of histochemistry and cytochemistry : official journal of the Histochemistry Society* 41: 733-743, 1993.
26. **Hancock CR, Brault JJ, and Terjung RL**. Protecting the cellular energy state during contractions: role of AMP deaminase. *Journal of physiology and pharmacology : an official journal of the Polish Physiological Society* 57 Suppl 10: 17-29, 2006.
27. **Hermansen L, and Osnes JB**. Blood and muscle pH after maximal exercise in man. *J Appl Physiol* 32: 304-308, 1972.
28. **Huxley HE, and Hanson J**. The structural basis of the contraction mechanism in striated muscle. *Annals of the New York Academy of Sciences* 81: 403-408, 1959.
29. **Iorga B, Adamek N, and Geeves MA**. The slow skeletal muscle isoform of myosin shows kinetic features common to smooth and non-muscle myosins. *The Journal of biological chemistry* 282: 3559-3570, 2007.
30. **Johansen KL, Doyle J, Sakkas GK, and Kent-Braun JA**. Neural and metabolic mechanisms of excessive muscle fatigue in maintenance hemodialysis patients. *American journal of physiology Regulatory, integrative and comparative physiology* 289: R805-813, 2005.
31. **Juel C, Bangsbo J, Graham T, and Saltin B**. Lactate and potassium fluxes from human skeletal muscle during and after intense, dynamic, knee extensor exercise. *Acta physiologica Scandinavica* 140: 147-159, 1990.
32. **Juel C, Klarskov C, Nielsen JJ, Krustrup P, Mohr M, and Bangsbo J**. Effect of high-intensity intermittent training on lactate and H+ release from human skeletal muscle. *American journal of physiology Endocrinology and metabolism* 286: E245-251, 2004.
33. **Karatzaferi C, Chinn MK, and Cooke R**. The force exerted by a muscle cross-bridge depends directly on the strength of the actomyosin bond. *Biophysical journal* 87: 2532-2544, 2004.
34. **Karatzaferi C, de Haan A, Ferguson RA, van Mechelen W, and Sargeant AJ**. Phosphocreatine and ATP content in human single muscle fibres before and after maximum dynamic exercise. *Pflugers Archiv : European journal of physiology* 442: 467-474, 2001.
35. **Karatzaferi C, de Haan A, van Mechelen W, and Sargeant AJ**. Metabolic changes in single human fibres during brief maximal exercise. *Experimental physiology* 86: 411-415, 2001.
36. **Karatzaferi C, Franks-Skiba K, and Cooke R**. Inhibition of shortening velocity of skinned skeletal muscle fibers in conditions that mimic fatigue. *American journal of physiology Regulatory, integrative and comparative physiology* 294: R948-955, 2008.
37. **Karatzaferi C, Myburgh KH, Chinn MK, Franks-Skiba K, and Cooke R**. Effect of an ADP analog on isometric force and ATPase activity of active muscle fibers. *American journal of physiology Cell physiology* 284: C816-825, 2003.

38. **Lanza IR, Wigmore DM, Befroy DE, and Kent-Braun JA**. In vivo ATP production during free-flow and ischaemic muscle contractions in humans. *The Journal of physiology* 577: 353-367, 2006.
39. **Macdonald WA, and Stephenson DG**. Effects of ADP on sarcoplasmic reticulum function in mechanically skinned skeletal muscle fibres of the rat. *The Journal of physiology* 532: 499-508, 2001.
40. **Månsson A**. Actomyosin-ADP States, Interhead Cooperativity, and the Force-Velocity Relation of Skeletal Muscle. *Biophysical journal* 98: 1237-1246, 2010.
41. **Margossian SS, and Lowey S**. Interaction of myosin subfragments with F-actin. *Biochemistry* 17: 5431-5439, 1978.
42. **Millar NC, and Geeves MA**. The limiting rate of the ATP-mediated dissociation of actin from rabbit skeletal muscle myosin subfragment 1. *FEBS letters* 160: 141-148, 1983.
43. **Nelson CR, Debold EP, and Fitts RH**. Phosphate and acidosis act synergistically to depress peak power in rat muscle fibers. *American journal of physiology Cell physiology* 307: C939-950, 2014.
44. **Nyitrai M, Rossi R, Adamek N, Pellegrino MA, Bottinelli R, and Geeves MA**. What limits the velocity of fast-skeletal muscle contraction in mammals? *Journal of molecular biology* 355: 432-442, 2006.
45. **Pate E, Bhimani M, Franks-Skiba K, and Cooke R**. Reduced effect of pH on skinned rabbit psoas muscle mechanics at high temperatures: implications for fatigue. *The Journal of physiology* 486 (Pt 3): 689-694, 1995.
46. **Pate E, and Cooke R**. Addition of phosphate to active muscle fibers probes actomyosin states within the powerstroke. *Pflugers Archiv : European journal of physiology* 414: 73-81, 1989.
47. **Reconditi M, Linari M, Lucii L, Stewart A, Sun YB, Narayanan T, Irving T, Piazzesi G, Irving M, and Lombardi V**. Structure-function relation of the myosin motor in striated muscle. *Annals of the New York Academy of Sciences* 1047: 232-247, 2005.
48. **Sahlin K, Harris RC, Nylind B, and Hultman E**. Lactate content and pH in muscle samples obtained after dynamic exercise. *Pflügers Archiv* 367: 143-149, 1976.
49. **Schiaffino S, and Reggiani C**. Fiber types in mammalian skeletal muscles. *Physiological reviews* 91: 1447-1531, 2011.
50. **Sieck GC, Fournier M, Prakash YS, and Blanco CE**. Myosin phenotype and SDH enzyme variability among motor unit fibers. *Journal of applied physiology* 80: 2179-2189, 1996.
51. **Siemankowski RF, Wiseman MO, and White HD**. ADP dissociation from actomyosin subfragment 1 is sufficiently slow to limit the unloaded shortening velocity in vertebrate muscle. *Proceedings of the National Academy of Sciences of the United States of America* 82: 658-662, 1985.
52. **Spudich JA, and Watt S**. The regulation of rabbit skeletal muscle contraction. I. Biochemical studies of the interaction of the tropomyosin-troponin complex with actin and the proteolytic fragments of myosin. *The Journal of biological chemistry* 246: 4866-4871, 1971.
53. **Tesi C, Colomo F, Nencini S, Piroddi N, and Poggesi C**. The effect of inorganic phosphate on force generation in single myofibrils from rabbit skeletal muscle. *Biophysical journal* 78: 3081-3092, 2000.
54. **Tesi C, Colomo F, Piroddi N, and Poggesi C**. Characterization of the cross-bridge force-generating step using inorganic phosphate and BDM in myofibrils from rabbit skeletal muscles. *The Journal of physiology* 541: 187-199, 2002.
55. **Toniolo L, Maccatrozzo L, Patruno M, Caliaro F, Mascarello F, and Reggiani C**. Expression of eight distinct MHC isoforms in bovine striated muscles: evidence for MHC-2B

presence only in extraocular muscles. *The Journal of experimental biology* 208: 4243-4253, 2005.
56. **Walklate J, and Geeves MA**. Temperature manifold for a stopped-flow machine to allow measurements from -10 to +40 degrees C. *Analytical biochemistry* 476: 11-16, 2015.
57. **Weeds AG, and Taylor RS**. Separation of subfragment-1 isoenzymes from rabbit skeletal muscle myosin. *Nature* 257: 54-56, 1975.
58. **Westerblad H, Allen DG, and Lannergren J**. Muscle fatigue: lactic acid or inorganic phosphate the major cause? *News in physiological sciences : an international journal of physiology produced jointly by the International Union of Physiological Sciences and the American Physiological Society* 17: 17-21, 2002.
59. **Westerblad H, Bruton JD, and Lannergren J**. The effect of intracellular pH on contractile function of intact, single fibres of mouse muscle declines with increasing temperature. *The Journal of physiology* 500 (Pt 1): 193-204, 1997.

Figures & Captions

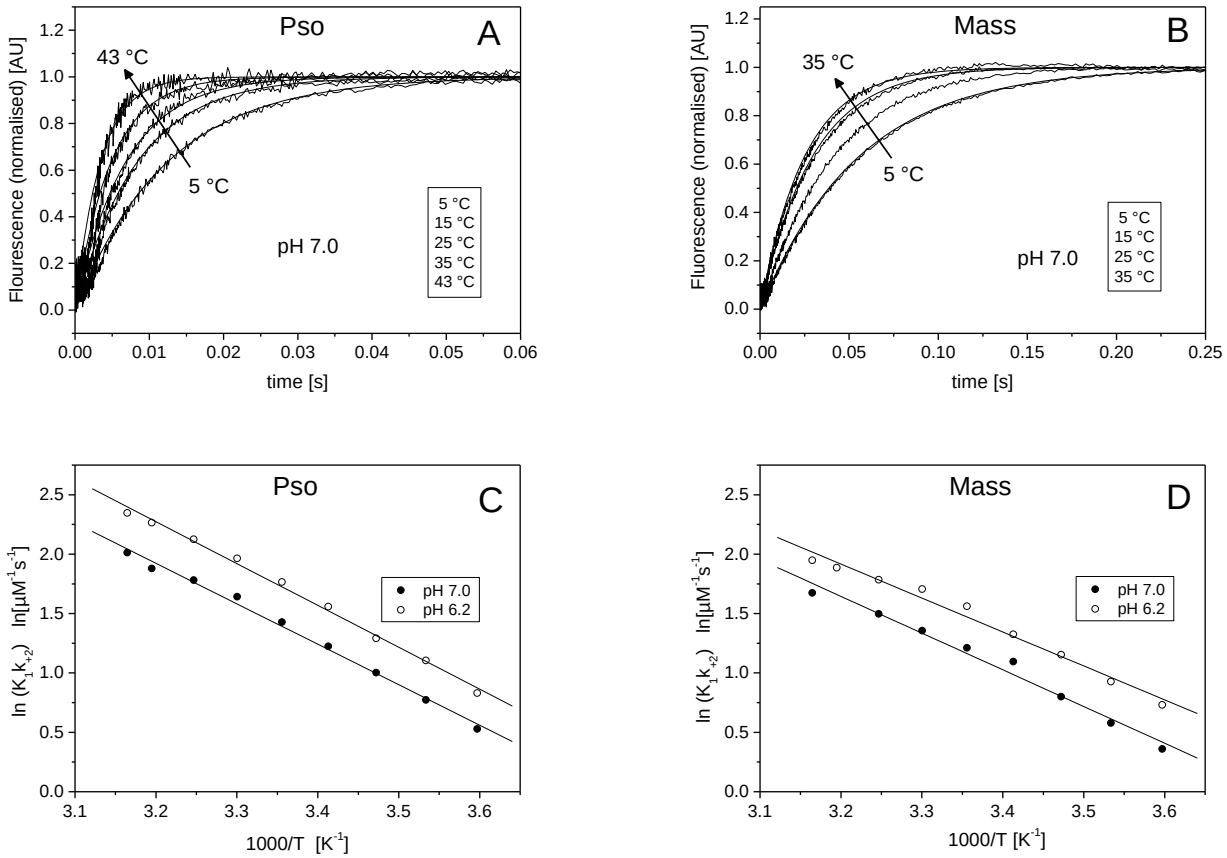

Figure 1. ATP-induced dissociation of S1 from actin, for fast (Pso) and slow (Mass) myosin isoform, at pH 7.0 and 6.2, in a range of temperatures. A. Normalized transients observed when mixing 0.5 μM pyr-act.PsoS1 with 25 μM ATP in pH 7.0 buffer at different temperatures (selected transients are shown). The change in fluorescence was fitted to a single exponential equation (best fits superimposed), giving k_{obs} of 84.8, 136.2, 208.5, 296.9, and 374.4 s^{-1} for 5, 15, 25, 35 and 43 °C, respectively. The amplitudes of the transients were relatively stable at 46 % of total fluorescence change, with some loss observed at temperatures above 30 °C. B. Normalized transients observed when mixing 0.5 μM pyrAct.MassS1 with 25 μM ATP in pH 7.0 buffer at different temperatures (selected transients are shown). The change in fluorescence was fitted to a single exponential equation (best fits superimposed), giving observed rate constants of 26.7, 36.1, 46.7, and 64.9 s^{-1} for 5, 15, 25 and 35 °C, respectively. The amplitudes of the transients were relatively stable at 40 % of total fluorescence change, with some loss observed at temperatures above 30 °C.C. Arrhenius plot of the $k_{obs}/[ATP]= K_1k_{+2}$ of Pso at pH 7.0 and pH 6.2 (temperature range 5 – 43 °C). The linear fits (best fits superimposed) gave slopes of -3.41 ±0.10 and -3.52 ±0.09 K for pH 7.0 and 6.2, respectively, from which the activation energies (Ea) were calculated as 28.3 ± 0.8 and 29.3 ± 0.8 kJ/mol. D. Arrhenius plot of the $k_{obs}/[ATP]= K_1k_{+2}$ of Mass at pH 7.0 and pH 6.2 (temperature range 5 – 43 °C). The linear fits (best fits superimposed) gave slopes of -3.09 ± 0.17 and -2.86 ± 0.14 K for pH 7.0 and 6.2, respectively, from which the activation energies (Ea) were calculated as 25.7 ± 1.4 and 23.8 ± 1.1 kJ/mol.

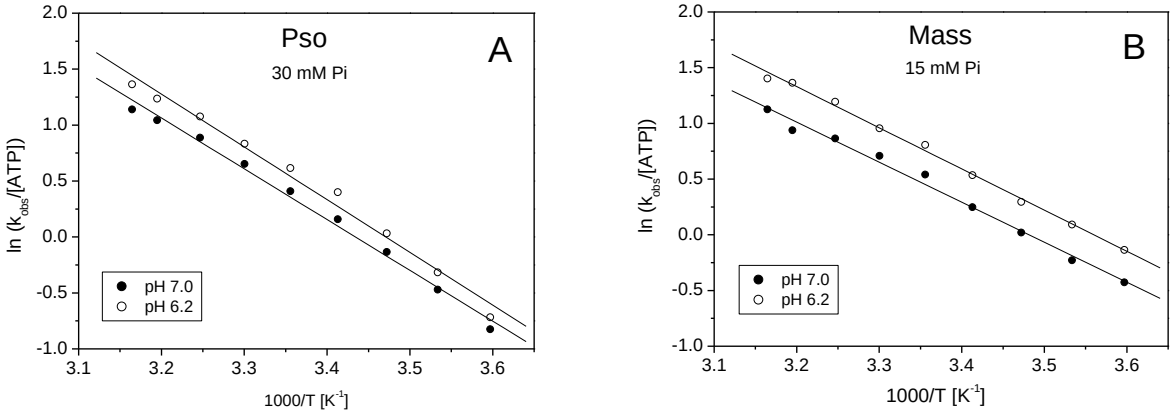

Figure 2. Effect of inorganic phosphate on the ATP-induced dissociation of S1 from actin, for fast (Pso) and slow (Mass) myosin isoform at pH 7.0 and 6.2, in a range of temperatures. A. Arrhenius plot of the k_{obs} of *Psoas* at pH 7.0 and pH 6.2 in the presence of 30 mM Pi. The linear fits (best fits superimposed) gave slopes of -4.54 ±0.15 and -4.71 ±0.20 K for pH 7.0 and 6.2, respectively, from which the activation energies (Ea) were calculated as 37.7 ± 1.2 and 39.2 ± 1.6 kJ/mol. B. Arrhenius plot of the k_{obs} of *Masseter* at pH 7.0 and pH 6.2 in the presence of 15 mM Pi. The linear fits (best fits superimposed) gave slopes of -3.59 ± 0.13 and -3.694 ± 0.08 K for pH 7.0 and 6.2, respectively, from which the activation energies (Ea) were calculated as 29.9 ± 1.1 and 30.7 ± 0.7 kJ/mol.

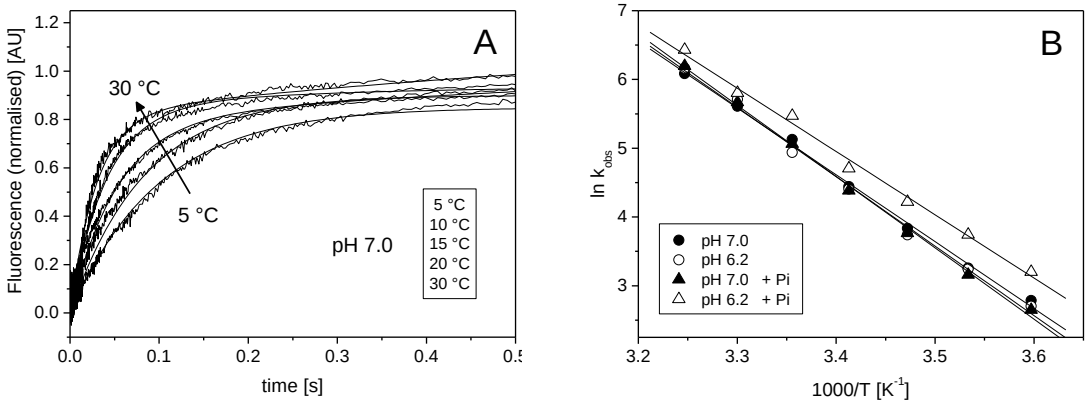

Figure 3. Temperature dependence of the ADP release from pyrAct.MassS1.A. Normalized fluorescent transients observed when 0.5 µM pyrAct.MassS1 pre-incubated with 75 µM ADP was mixed with 8 mM ATP at different temperatures between 5 and 30 °C in pH 7.0 buffer (selected transients are shown). The change in fluorescence was biphasic when observed over a time scale of 5 sec, however here only the initial fast phase is shown (fits superimposed). The k_{obs} for the fast phase were 16.2, 26.0, 46.3, 85.0 and 273 s^{-1} for 5, 10, 15, 20 and 30 °C, respectively. B. Arrhenius plot of the k_{obs} of the ADP release rate constant of *Masseter* at pH 7.0 and pH 6.2 in the absence and presence of 15 mM Pi. The linear fits (best fits superimposed) gave slopes of -9.72 ± 0.24 and -10.09 ± 0.33 K for pH 7.0 and 6.2, and -10.36 ± 0.23 and -9.20 ± 0.31 K for pH 7.0+Pi and pH 6.2 +Pi, respectively. The activation energies (Ea) were calculated as 75.9 ± 4.1 and 84.7 ± 6.1 kJ/mol for pH 7.0 and 6.2 without phosphate, and 94.4 ± 5.0 and 88.9 ± 3.9 kJ/mol for pH 7.0 and pH 6.2 respectively in the presences of phosphate.

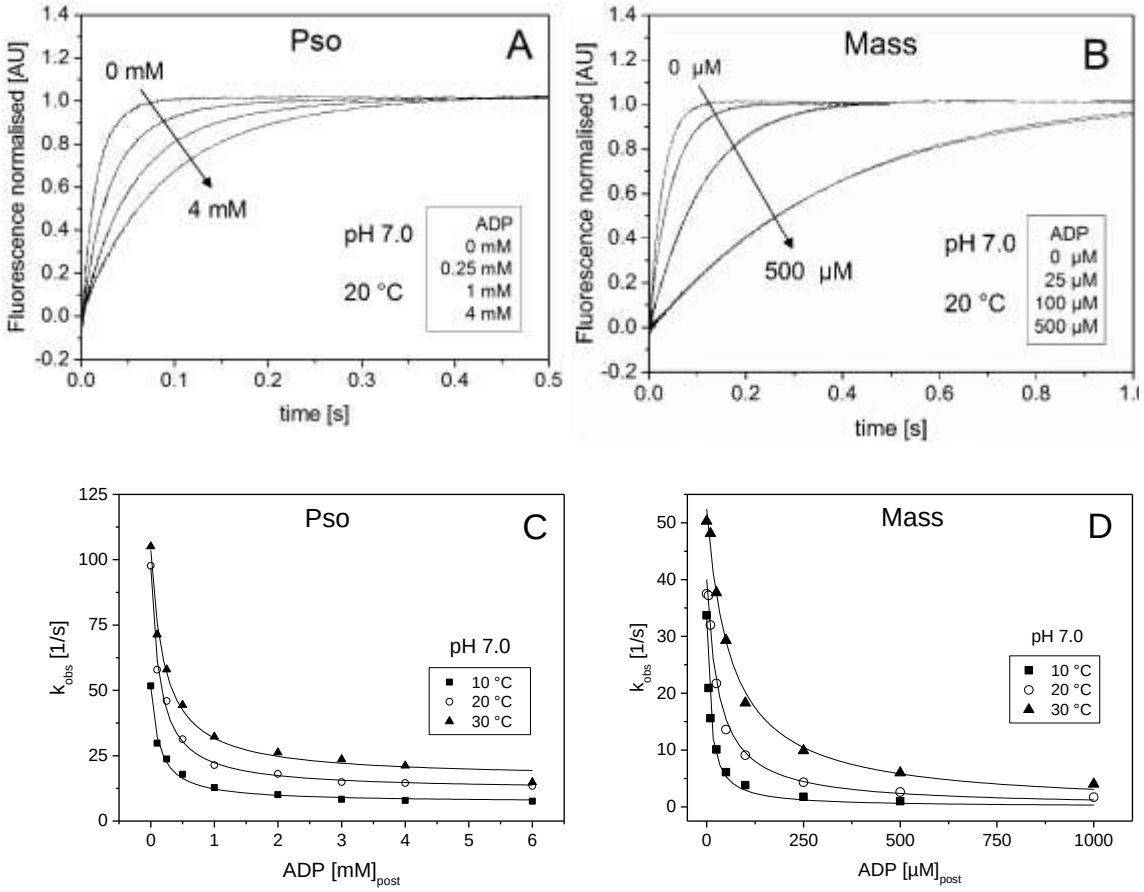

Figure 4. Temperature dependence of the ADP dissociation constant (K_{ADP}) for fast (Pso) and slow (Mass) A.S1 at pH 7.0. A. Normalized fluorescent transients observed when 0.5 µM pyrAct.PsoS1 was mixed with 25 µM ATP with various concentrations of ADP present at 20 °C in pH 7.0 buffer. The change in fluorescence was fitted by a single exponential equation (best fits superimposed). The k_{obs} determined were 87.7, 45.9, 21.4 and 14.5 s^{-1} for zero, 0.25, 1 and 4 mM ADP, respectively, with an amplitude of 30 % of total fluorescence. B. Fluorescent transients observed when 0.5 µM pyrAct.MassS1 was mixed with 25 µM ATP with various concentrations of ADP present at 20 °C in pH 7.0 buffer. The change in fluorescence was fitted to a single exponential equation (best fits superimposed). The k_{obs} determined were 37.5, 21.7, 9.1 and 2.6 s^{-1} for zero, 25, 100 and 500 µM ADP, respectively, with an amplitude of 30 % of total fluorescence. C. Plot of the observed rate constants as a function of [ADP] for *Psoas* in pH 7.0 buffer at 10, 20 and 30 °C. The data sets were fitted to a hyperbole to obtain the ADP dissociation constant (K_{ADP}) for each temperature: 131 ± 16 µM (10 °C), 140 ± 14 µM (20 °C) and 213 ± 29 µM (30 °C) for the depicted data. Refer to Table 1 for average values for from measurements in different days. D. Plot of the observed rate constants as a function of [ADP] for *Masseter* in pH 7.0 buffer at 10, 20 and 30 °C. The data sets were fitted to a hyperbole to obtain the ADP dissociation constant (K_{ADP}) for each temperature: 9.6 ± 0.7 µM (10 °C), 31.3 ± 4.0 µM (20 °C) and 62.4 ± 6.1 µM (30 °C) for the depicted data. Refer to Table 1 for average values from measurements in different days.

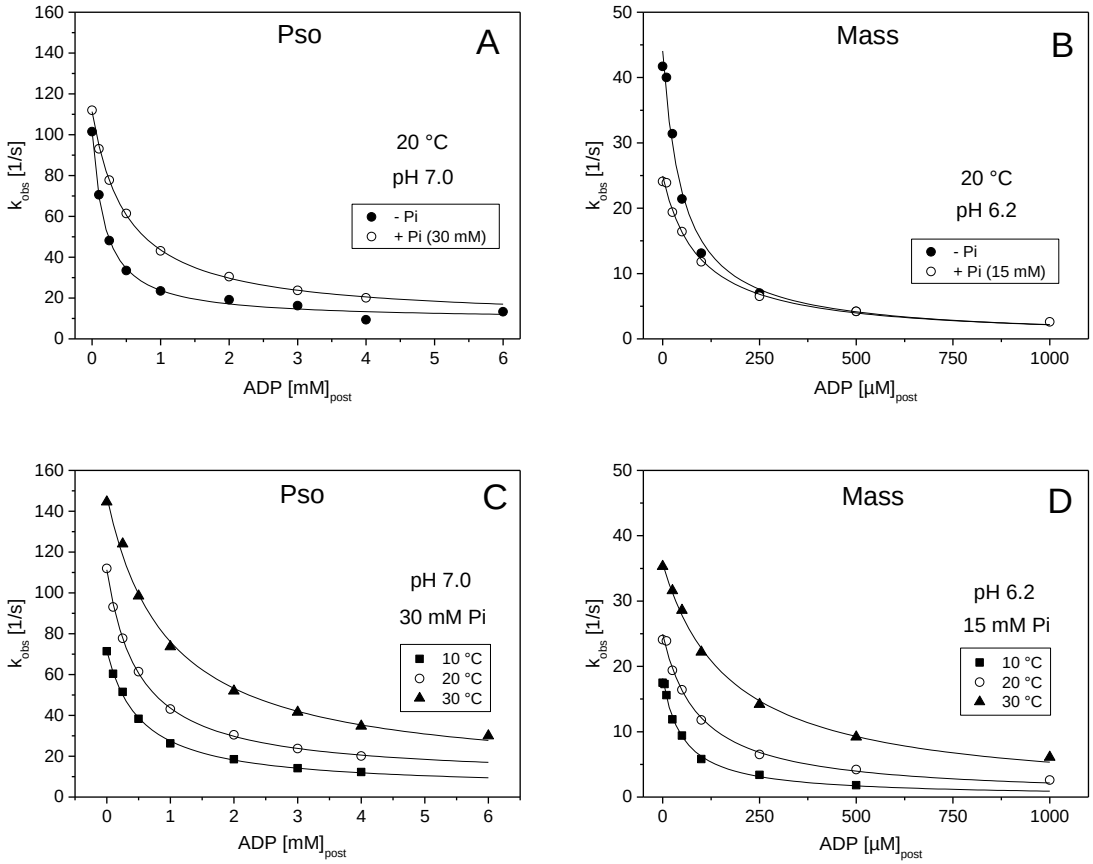

Figure 5. Effect of phosphate (Pi) on the K_{AD} of fast (Pso) and slow (Mass) A.S1. A. Plot of the observed rate constants as a function of [ADP] for *Psoas* in the presence and absence of added 30 mM Pi (pH 7.0 buffer at 20 °C). The data sets were fitted to a hyperbole to obtain the ADP dissociation constant (K_{ADP}) ± Pi: 175 ± 22 µM (no Pi) and 510 ± 22 µM (with Pi). Refer to Table 1 for average values for from measurements in different days. B. Plot of the observed rate constants as a function of [ADP] for *Masseter* in the presence and absence of added 15 mM Pi (pH 6.2 buffer at 20 °C). The data sets were fitted to a hyperbole to obtain the ADP dissociation constant (K_{ADP}) ± Pi: 48.4 ± 6.8 µM (no Pi) and 94.5 ± 8.1 µM (with Pi). Refer to Table 1 for average values for from measurements in different days. C. Plot of the observed rate constants as a function of [ADP] for *Psoas* in pH 7.0 buffer in the presence of added 30 mM Pi at 10, 20 and 30 °C. The data sets were fitted to a hyperbole to obtain the ADP dissociation constant (K_{ADP}) for each temperature: 530 ± 36 µM (10 °C), 510 ± 22 µM (20 °C) and 942 ± 117 µM (30 °C). Refer to Table 1 for average values for from measurements in different days. D. Plot of the observed rate constants as a function of [ADP] for *Masseter* in pH 6.2 buffer in the presence of added 15 mM Pi at 10, 20 and 30 °C. The data sets were fitted to a hyperbole to obtain the ADP dissociation constant (K_{ADP}) for each temperature: 52.2 ± 5.8 µM (10 °C), 94.5 ± 8.1 µM (20 °C) and 175.3 ± 9.7 µM (30 °C). Refer to Table 1 for average values for from measurements in different days.

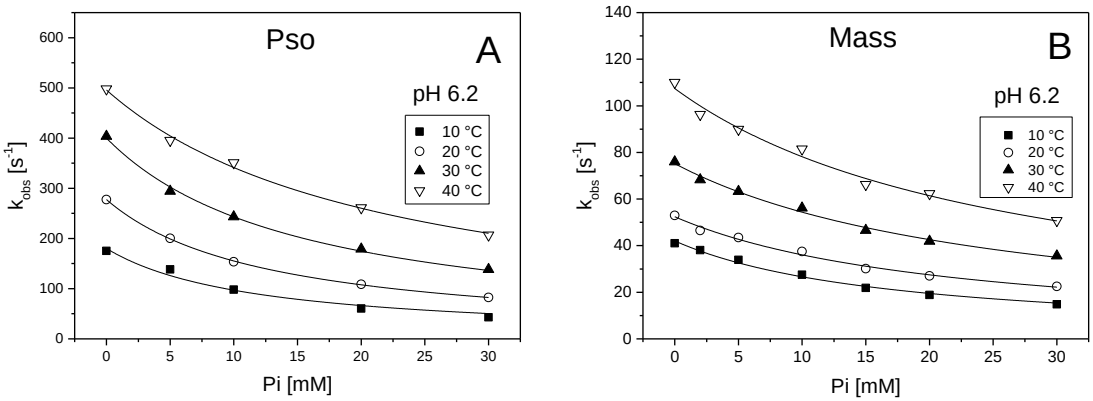

Figure 6. Phosphate (Pi) dissociation constant for A.M in the absence of ADP (phosphate) at pH 6.2, for fast (Pso) and slow (Mass) myosin isoform. A. Plot of the observed rate constants of the ATP-induced dissociation of 0.5 µM pyrAct.S1 by 50 µM ATP as a function of [Pi] for *Psoas* (pH 6.2 buffer) at 10 to 40 °C. The data sets were fitted to a hyperbole to obtain the Pi dissociation constant (K_{Pi}) for each temperature: 11.7 ± 1.8 mM (10 °C), 12.7 ± 0.2 mM (20 °C), 15.5 ± 0.7 mM (30 °C) and 22.1 ± 1.2 mM (40 °C). Refer to Table 1 for average values for from measurements in different days. B. Plot of the observed rate constants of the ATP-induced dissociation of 0.5 µM pyrAct.S1 by 25 µM ATP as a function of [Pi] for *Masseter* (pH 6.2 buffer) at 10 to 40 °C. The data sets were fitted to a hyperbole to obtain the Pi dissociation constant (K_{Pi}) for each temperature: 17.3 ± 1.1 mM (10 °C), 22.0 ± 1.4 mM (20 °C), 26.1 ± 1.3 mM (30 °C) and 26.7 ± 2.1 mM (40 °C). Refer to Table 1 for average values for from measurements in different days.

827 **Tables**

828 **Table 1.** Average values of kinetic parameters describing the ATP induced
829 dissociation rate of actin.S1 for psoas and masseter myosin, in pH 7 and 6.2, under
830 different temperatures, in the absence or presence of added phosphate.

831

832

833

834

835 **Table 2.** Thermodynamics results (E_A values) describing the temperature
836 dependence of the dissociation rate constant for psoas (Pso) and masseter (Mass)
837 myosin, under pH 7 and 6.2.

838

839

840

Modulators of actin-myosin dissociation: basis for muscle type differences in contraction during fatigue

104 characters incl. spaces

Authors: Christina Karatzaferi [1,2], Nancy Adamek [3], and Michael A. Geeves [3]

[1] Muscle Physiology and Mechanics Group, DPESS, University of Thessaly, Karyes, Trikala, 42100, Greece

[2] Experimental Myology and Integrative Biology Cluster, FSHS, University of St Mark and St John UK

[3]School of Biosciences, University of Kent, Canterbury, CT2 7NH Kent, UK

Running head: Muscle type actomyosin dissociation differences in fatigue

58 characters incl. spaces

Address for correspondence: M.A. Geeves, School of Biological Sciences, University of Kent, Canterbury, CT2 7NH Kent, UK M.A.Geeves@kent.ac.uk

Author contributions: CK & MAG conceived the study, MAG & CK designed the study, NA & CK collected data, NA created figures and tables, all co-wrote and edited the paper.

Abstract

The muscle types present with variable fatigue tolerance, in part due to the myosin isoform expressed. However, the critical steps that define 'fatigability' *in vivo* of fast vs slow myosin isoforms, at the molecular level, are not yet fully understood. We examined the modulation of the ATP-induced myosin sub-fragment 1 (S1) dissociation from pyrene-actin by inorganic phosphate (Pi), pH and temperature using a specially modified stopped-flow system (HiTech Scientific SF-61DX2) that allowed fast kinetics measurements at physiological temperature. We contrasted the properties of rabbit psoas (fast) and bovine masseter (slow) myosins (obtained from samples collected from New Zealand rabbits and from a licensed abattoir, respectively, according to institutional and national ethics permits). To identify ATP cycling biochemical intermediates, we assessed ATP binding to a pre-equilibrated mixture of actomyosin and variable [ADP], pH (pH 7 vs pH 6.2) and Pi (zero, 15 or 30 added mM Pi) in a range of temperatures (5 to 45^{o}C). Temperature and pH variations had little, if any, effect on ADP affinity (K_{ADP}) for fast S1 but for slow S1 K_{ADP} was weakened with increasing temperature or low pH. In the absence of ADP, affinity for phosphate (K_{Pi}) was weakened with increasing temperature for fast S1. In the presence of ADP, myosin type differences were revealed at the apparent phosphate affinity, depending on pH and temperature. Overall, the data point to distinct mechanochemical coupling differences between myosin types which could help explain the *in vivo* observed muscle types differences at rest and during fatigue.

248 words

Keywords: myosin kinetics, cross-bridge cycle, mechanochemical coupling, temperature, muscle fatigue

Introduction

Mammalian striated muscle contraction depends directly on the interaction of the motor protein myosin II, organized in multi-headed filaments, with the filamentous 'tracks' of actin, all arranged along with other proteins into sarcomeres, the 'functional units' of muscle (23, 38). In essence whole muscle force output eventually depends on the number of myosin cross bridges interacting 'strongly' or 'weakly' with actin, while the velocity of contraction depends on the rate at which myosin detaches from actin at the end of the working stroke (8).

Peripheral muscle fatigue is manifested by a transient reduction in work or power output induced by physical exertion. Depression of muscle power comes as a result of force decline and the slowing of contraction velocity and is accompanied by biochemical alterations of the intracellular milieu (9, 18). Because the decline in force can be accompanied by a relatively larger reduction of energy turnover (i.e. tension economy, observed in *in situ* (19) or isolated intact muscle models (13), fatigue could be also viewed as a physiological protective mechanism 'saving' the tissue from a potential energetic crisis. At the organismal level, fatigue is revealed to be a complex multifaceted phenomenon, with a large heterogeneity of research outcomes (4) depending, among other factors, on the type, duration and intensity of muscular activity employed (5, 7), the muscle composition studied (22) and health status (25). Still, recovery of the muscle's performance capacity is observed with adequate rest, this being a 'criterion' of physiological peripheral fatigue. At the muscle cellular level, changes in muscle mechanics during fatigue could be related to either reduction of energy substrates (e.g. causing localized ATP minima (27, 28)) and /or accumulation of ATP hydrolysis by-products (e.g. (11, 26, 30, 36, 43)). This is because the interaction of myosin with actin (actomyosin) is not only fueled by ATP hydrolysis but it is also modulated by ATP hydrolysis by-products (ADP, Pi, H+) and other prevailing intracellular conditions (9). Thus, at the myofibrillar level, and for the purposes of this work, fatigue is considered in the context of factors influencing the actomyosin cycle in a way to cause slowing of the cycle and/or weaker actomyosin interactions.

The coupling of biochemical steps with mechanical events has, however, not been fully elucidated (20) while the 'laws' governing how large ensembles of myosins integrate within the organized sarcomere (16, 17, 31) are not yet fully defined. Investigations ranging from whole body exercise (5, 25), to intact small muscles or fibers (48) to skinned fibers, (10, 11, 15, 26, 30, 37) or myofibrils (43), and isolated molecule approaches (14) have provided strong evidence that the accumulation of inorganic phosphate (Pi) and of hydrogen ions can contribute to, if not cause, peripheral muscle fatigue. Still, their exact impact, especially at physiological *in vivo* conditions, has attracted much debate (e.g. (47)). This is further complicated by muscle type differences (fast vs slow) in energetics, myosin ATPase, and mechanical performance (6, 39, 40) , which can be linked to a great degree to inherent properties of the myosin II isoform expressed.

Myosin II exists in multiple isoforms (39) with *slow* muscles expressing the type 1 (MyHC-1 also known as β myosin) and *fast* muscles expressing one or more of the type 2 myosins (MyHC-2a, 2b, or 2x). The study of kinetics of the actomyosin (A.M) interaction cycle identifies clear intermediate steps (for a review see (3)). Such studies have revealed that slow skeletal myosin heavy chain isoforms (MyHC 1) have distinct properties from fast isoforms (MyHC 2s) with regards not only to the ATPase activity but also to the rate and equilibrium constants of the various biochemical steps of the pathway which are expected to dictate their different mechanical properties. For example, efficiency of actin induced ADP displacement from myosin (the ratio of ADP affinity for A.M (K_{AD}) over the ADP affinity for myosin (K_D)), and strain sensitivity (dependence on external mechanical load) can differ substantially between fast and slow myosins (3, 20) , with slow myosins binding ADP tightly and releasing it at a slower rate than fast myosins. Thus, it is considered that the ADP release is the rate limiting step for the maximum contraction velocity of slow muscles (24, 35), at least at the temperatures where fibers or myosin solutions are usually studied (10 to 22 °C).

However, *in vivo* mammalian muscle temperature ranges from 32 to > 40 °C, while in severe fatigue, pH drops and inorganic phosphate (Pi) accumulates (21). A number of *in vitro* fiber studies at higher temperatures, have challenged long held views about

the individual role of the key 'fatigue' metabolites on mechanics, e.g. low pH on force (less of an effect (29, 36, 48)), high Pi on force (less of an effect, (10, 11, 15, 26)). More importantly, it appears that a higher temperature is necessary to tease out physiological synergies; e.g. in skinned fibers, a synergism of myosin light chain phosphorylation with low pH and high [Pi] in slowing contraction velocity and repressing power output became evident only in experiments performed at a high temperature (29) . Overall, many studies now indicate that temperature considerations and a holistic, systems, approach are crucial if one wants to realistically link muscle function *in vivo* to actomyosin interaction molecular events studied *in vitro*.

The steps that control the detachment of the myosin cross-bridge at the end of the working stroke from actin are rapid and are thought to limit the shortening velocity, a key parameter of muscle function. Temperature predictions from kinetic studies of actomyosin in solution (35), suggest that the rate of ADP release may limit unloaded velocity for both isoforms. It can be hypothesized that such an ADP effect could be aggravated by the presence of hydrogen ions and inorganic phosphate, as in fatigue.

Therefore the purpose of this research was to study the fast kinetics of ATP-induced dissociation of A.M. with and without ADP using the stopped flow. We examined the interplay of 'fatigue' factors, e.g. low pH and high inorganic phosphate (Pi), with myosin type, on ATP-induced dissociation of A.M. Taking advantage of recent methodological advancements we studied, for the first time, the ATP-induced dissociation of fast and slow S1 from actin in temperatures ranging from 5 to 45 ^{o}C to reveal critical myosin type and/or temperature dependencies of these processes.

Glossary & abbreviations

A.M: actomyosin complex
S1: myosin subfragment 1
actin.S1: actin bound with S1
K_1 : equilibrium constant for the formation of the complex of AM with ATP (denoted as A.M.T),

k_{+2}: rate constant of isomerization of A.M.T to A-M.T which is followed by actin dissociation
k_{obs}: observed rate constant of ATP induced dissociation of myosin from actin
K_{ADP}: affinity for ADP
K_{Pi}: affinity for phosphate
K_{ADP+Pi}: affinity for ADP in the presence of phosphate
MyHC: myosin heavy chain

Materials and methods

Ethics Statement

Muscle tissue was obtained post-mortem from animals treated as recommended by national and local guidelines (UK Animals (Scientific Procedures) Act, 1986). Fast skeletal muscle came from the psoas muscle of New Zealand rabbits and slow skeletal muscle from bovine masseter.

Protein preparation

Myosin was prepared from the rabbit psoas (for fast MyHC-II) and the bovine masseter muscle (for slow MyHC-I) according to Margossian and Lowey (32) , and was subsequently digested to subfragment 1 (S1) with chymotrypsin as described by Weeds & Taylor (46) . Actin was prepared from rabbit muscle as described by Spudich & Watt (42) and labelled with pyrene iodoacetamide to give pyrene-labelled actin as described by Criddle et al (12). Protein stocks of S1 and of pyrene-labelled actin were stored at 4^{o}C and were used for up to 2 weeks. In the text herein reference to actin implies pyrene-labelled actin.

Experimental buffers

The main buffer contained 20 mM cacodylate (adjusted at pH 7.0 or pH 6.2), 100 mM KCl, 5 mM $MgCl_2$ and 1 mM NaN_3; when phosphate was present in the buffer the ionic strength was adjusted accordingly to a final ionic strength of 170 mM. Concentrations (whether of proteins or buffer constituents) given in the text and figure legends refer to the concentration after mixing 1:1 in the stopped flow (unless stated otherwise).

Experimental equipment and procedures

Stopped-flow experiments were performed essentially as described previously (2) using a HiTech Scientific SF-61DX2 stopped flow system and 4-5 transients were acquired for each ATP transients (Kinetic Studio suite). The dead time of the equipment was 0.002 s. A wide temperature range (5 – 45 ^{o}C) for measurements was available because of a new adaptation of the standard stopped flow machine (see (45)). Briefly, the drive syringes were held at room temperature (20 °C) while loading lines leading into the mixing chamber, the mixing and observation chamber were all thermostated at the temperature of the measurement. Essentially the samples were only exposed to the temperature of the measurement for a few seconds, thus allowing measurements of proteins under conditions where they are not usually stable for long.

The **ATP induced dissociation rate of actin.S1**, was measured in the stopped-flow by mixing a fixed concentration of pyr.actin.S1 complex (end concentration 0.25 μM) with excess ATP and monitoring fluorescence transients from the pyrene-labeled actin (excitation at 365 nm, emission through a KV389 nm cut-off filter (Schott, Mainz, Germany)).

In a similar process, **ADP affinity** (K_{ADP}) was measured by adding ADP as a competitive inhibitor of ATP. In this case 0.5 μM pyr.actin.S1 was mixed with 25 μM ATP with various concentrations of ADP present with the ATP (from 0 to 1200 μM).

Phosphate affinity (K_{Pi}) was measured exactly as for the ADP affinity except that the high concentrations of Pi used meant it was more convenient to have P_i present in the buffer in both syringes of the stopped-flow.

ADP affinity in the presence of phosphate (K_{ADP+Pi}) was also measured using the same approach as for K_{ADP} but using buffers containing fixed amounts of inorganic phosphate, 30 mM in the case of psoas S1 and 15 mM with masseter S1. The different affinities of Pi for the two types of S1 required a different concentration of Pi.

Experiments were performed at two pH levels, 7 and 6.2 and in a range of temperatures. Care was taken to reverse the order of experiments to avoid the possibility of a time and 'order' effect either with respects to pH or temperature.

Data Fitting and Interpretation Approach

In the present study we focused our attention on the ATP induced dissociation of actin.S1. This is the step that controls the detachment of the actomyosin cross-bridge at the end of the working stroke.

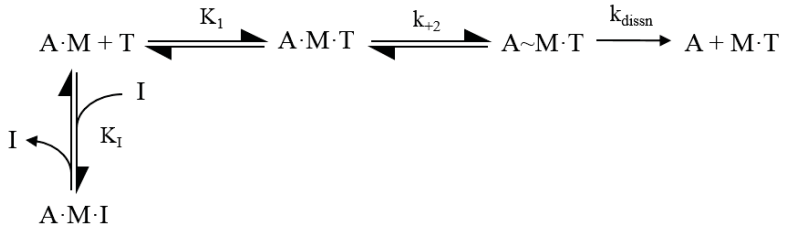

Scheme 1. Model of ATP-induced dissociation of actin.S1 based on Millar and Geeves (33) .

In Scheme 1, T = ATP; A = actin; M = myosin; I is an inhibitor, competitive with ATP for the nucleotide binding site. K_1 defines the equilibrium constant for the formation of the A.M.T collision complex, which is followed by an almost irreversible isomerization of the complex to the ternary complex A-M.T with the rate constant of k_{+2}. This is rapidly followed by dissociation of actin from the ternary complex. K_I is defined as a dissociation constant k_{+I}/k_{-I}. In the experiments presented here the inhibitor was either ADP or inorganic phosphate (P_i).

The reaction described in Scheme 1 was monitored through pyrene fluorescence changes which monitor the ATP induced dissociation of actin from the complex (fluorescence increases by up to 70 %.), specifically associated with step 2 of Scheme 1, (see in Results, Fig. 1A). Four to five transients were collected for each ATP concentration used then averaged before further analysis.

The averaged transients were fitted with single (eqn1) or, if needed, a double exponential equation (eqn2):

$$F_t = \Delta F \cdot e^{(-k_{obs} \cdot t)} + F_\infty \qquad \textit{eqn 1}$$

or

$$F_t = \Delta F_{(1)} \cdot e^{(-k_{obs(1)} \cdot t)} + \Delta F_{(2)} \cdot e^{(-k_{obs(2)} \cdot t)} + F_\infty \qquad \textit{eqn 2}$$

Where F_t is the observed fluorescence at time t, F_∞ is the fluorescence at the end of the transient (t= ∞) and ΔF is the total change of fluorescence observed. The observed rate constant (k_{obs}) reflects the ATP induced dissociation rate of actin.S1 and is linearly dependent on [ATP], at the ATP concentrations used here. A plot of [ATP] vs k_{obs} was used to derive the values of K_1 and k_{+2} (using Origin v 6.0), as defined in scheme 1 and eqn 3.

$$k_{obs} = K_1 k_{+2}[ATP] \qquad \textit{eqn 3}$$

The presence of a competitive inhibitor to ATP binding (that does not induce actin.S1 dissociation) would appear to slow the rate of actin.S1 dissociation. If inhibitor binding is in rapid equilibrium with actin.S1, within the timescale of data acquisition, compared to the rate of ATP-induced dissociation of actin.S1 (i.e. $k_{+AD} + [ADP]k_{-AD} >> K_1 k_{+2}[ATP]$) , then

$$k_{obs} = K_1 k_{+2}[ATP]/(1 + ([ADP]/K_I)) \qquad \textit{eqn 4}$$

Then, plotting k_{obs} as a function of [I] will allow the K_I (in scheme 1) to be defined. This approach was used to define the value of K_I for ADP (K_{AD}) and Pi (K_{Pi}).

If both ADP and Pi are present in the same measurement, two scenarios are possible. If both compete for the same binding site then the effect of the two inhibitors is additive and the effect on k_{obs} can be predicted from the values of K_{AD} and K_{Pi} measured independently.

$$k_{obs} = K_1 k_{+2}[ATP]/(1 + ([ADP]/K_{AD}) + ([Pi]/K_{Pi})) \quad \text{eqn 5}$$

where the measured K_I at fixed [Pi] as in $K_I = 1/K_{AD} + [Pi]/K_{Pi}$

If both however bind into the ATP pocket at the same time to create the complex A.M.ADP.Pi then the above relationship will not hold and Pi will alter the affinity of

A.M for ADP.

The apparent affinity of ADP for actin.S1 ($K_{ADP.Pi}$) was measured for several concentrations of Pi and then the affinity of Pi calculated according to the following relationship and compared with the value of $K_{PI.}$

$$K_{Pi\ app} = [Pi]/(K_{ADP+Pi}/K_{ADP} – 1) \qquad \text{eqn 6}$$

ADP release rate constant. Two types of myosins were studied which are known to differ in their affinity for nucleotides (3, 41). The rate constant for the release of ADP (k_{-ADP}) is relatively slow and can easily be measured in an ADP displacement experiment. This step is very fast for a fast muscle isoform and too fast to measure by current equipment. Briefly, actin.^{Mass}S1 saturated with 75 µM of ADP (A.M.D complex) was mixed with a large excess of ATP (8 mM) in the stopped-flow. Then the k_{obs} values, fitted to a single exponential equation (eqn 1) defined the rate constant by which ADP is released by the ternary A.M.D complex (k_{-AD}).

The data presented in the figures are the values for the individual experiment displayed, while the data values presented in the table 1 are averaged values for n = independent day measurements.

The *temperature dependence* of the above studied biochemical steps K_1k_{+2}, K_{AD}, K_{Pi} and $K_{ADP\ Pi}$ data were plotted as the natural logarithm of the measured parameter against the reciprocal of temperature in degrees Kelvin ($1/T\ ^oK$) and fitted with linear regression using the Arrhenius (rate constants) or vant Hoff (equilibrium constants) equations

$$\ln K_1k_{+2} = \ln (A) - Ea/RT \qquad \text{eqn 7}$$

$$\text{Ln Keq} = \Delta S°/R - \Delta H°/RT \qquad \text{eqn 8}$$

where Ea stands for activation energy, R is the gas constant, A is a pre-exponential factor. The values of –Ea/R or or $\Delta H°/R$ were derived from the slopes.

Results & Discussion

ATP induced dissociation rate of actin.S1. When Actin.^{Pso}S1 and actin.^{Mass}S1 were mixed with ATP, as shown in Figure 1 A and B, the observed stopped-flow transients were described by a single exponential for both myosin isoforms (Fig 1A and 1B). Keeping a fixed ATP concentration and increasing the temperature allows the best estimate of the temperature dependence of the reaction since it minimizes variation in ATP concentration between experiments. Increasing the temperature from 5-43 °C reduced the total fluorescence signal by ~ 40% due to collisional quenching but the signal change remained relatively constant with an approximately 2-fold increase in fluorescence observed in all transients. The transients were therefore normalized to illustrate the change in the k_{obs} values. For *psoas* (Fig 1 A) and *masseter* (Fig 1 B) temperature increased the k_{obs} value ~3 fold in both cases over the range of measurements from 3 to 43 °C. The figure shows illustrative examples of one set of transients.

Lowering the pH to 6.2 slightly increased the k_{obs} values for both isoforms by about 20-25 % (and hence the second order rate constant $K_1k_{+2,}$ see Table 1). Increasing temperature resulted in an average increase of 3 fold over the temperature range of 5-35 °C. The amplitudes of the transients at pH 6.2 were again relatively stable and similar to pH 7 for ^{Pso}S1 at 43 %. For ^{Mass}S1 the amplitudes were also stable in pH 6.2 but showed an overall increase in fluorescence from 40 to 50% of total fluorescence signal.

Effect of temperature: The temperature dependence of the dissociation rate constant was examined at pH 7 and then repeated at pH 6.2 (Fig 1C and 1D). Each measurement was repeated 3 times and the average values collated in Table 2. The Arrhenius plots of the temperature dependence measurements at pH 7 and 6.2 gave well defined straight lines over the temperature range (5 – 43 ^{o}C). In the absence of phosphate, for *psoas* the activation energy (Ea) values were very similar at pH 7.0 and 6.2 as shown in Figure 1 C, 28.3 ± 0.8 and 29.3 ± 0.8 kJ/mol respectively. For masseter, Ea values were on average lower than the ones for fast, being for pH 7.0 and 6.2, 25.7 ± 1.4 and 23.8 ± 1.1 kJ/mol respectively (Figure 1D).

Effect of Pi and pH: When the ATP-induced dissociation measurements were repeated in the presence of high phosphate concentrations, of the order that might be expected in fatigue, the observed rate constants for the dissociation reaction were 2-fold slower for ^{Mass}S1 and 2- to 3-fold slower for ^{Pso}S1 at both pH levels compared to the data in the absence of phosphate. This is consistent with Pi acting as a competitive inhibitor with a K_i of 10 – 20 mM. It should be noted that while 30 mM Pi was used for ^{Pso}S1, 15 mM Pi was used for ^{Mass}S1 experiments.

The transients of both isoforms had bi-phasic tendencies at the low temperatures (5-10 °C) at both pHs, but were single exponential at all other temperatures. The origin of this additional slow phase, which had a very small amplitude (1-3 %), is not known, but possible contamination by ADP was eliminated by control measurements in the presence of apyrase.

The amplitudes of the dissociation reaction were 50 % smaller/reduced in the presence of phosphate for both, ^{Pso}S1 and ^{Mass}S1, indicating some loss of affinity of S1 for actin in the presence of Pi. However, for psoas the amplitudes increased with temperature from 25 to 30 % at pH 7.0 and even more dramatically from 12 to 20 % at pH 6.2. This behavior was not observed with ^{Mass}S1 *masseter*.

Combined effect of temperature, pH and phosphate: the temperature dependence of the dissociation rate constant in the presence of phosphate is shown in Figure 2 and the activation energies determined for *psoas* (38 ± 1 kJ/mol) and *masseter* (30 ± 1 kJ/mol) were greater than in the absence of Pi, irrespective of the pH used. Thus phosphate increased the activation energy of ^{Pso}S1 at both pH values by about 10 kJ/mol, which is a larger increase than observed with *masseter*, where the increase was only about 5 kJ/mol in the presence of phosphate.

Rate constant of ADP release (k_{-ADP}) was evaluated by an ADP displacement experiment, mixing actin.^{Mass}S1 saturated with ADP with an excess of ATP. This measurement was not possible for ^{Psoas}S1 because the ADP release is too fast to measure.

Displacement of ADP from actin.^{Mass}S1 by a large excess of ATP was biphasic. The transients were well-defined with stable amplitudes of 24 and 6 % for the fast and slow phase, respectively (as shown in Figure 3 A). These amplitudes were similar under all conditions explored. The fast phase defines the rate constant at which ADP is released and is thought to limit the velocity of shortening of a masseter muscle (2). The slower phase is an off pathway event and will not be considered further here. The k_{obs} of the ADP release was 85 s^{-1} at 20 °C (pH 7.0) and compares well to published results of 94 s^{-1} by Bloemink et al (2).

The reaction was measured over the temperature range of 5 - 30 °C at pH 6.2 and 7.0, and in the presence of 15 mM Pi. The k_{obs} values are summarized in the Arrhenius plot in Fig 3B. The k_{obs} values increased from 16.2 at 5 °C to 273 s^{-1} at 30 °C with similar values at pH 7.0 and pH 6.2 throughout the temperature range used. Above 30 °C the reaction was too fast to measure reliably. Thus the activation energy was large with similar values at both pH levels studied.

The addition of 15 mM Pi had little effect at pH 7.0. At pH 6.2 however we saw a 30-50 % increase in k_{obs} in the presence of phosphate and a small change in the activation energy.

ADP affinity (K_{ADP})

The ADP affinity (K_{ADP}) for pyr.actin.S1 was measured by the competitive inhibitor approach as described in the Methods.

ADP included in the ATP solution competes with ATP for binding to the pyr.actin.S1 and slows the k_{obs} value as shown in Fig 4. The ADP affinity was 168 µM for ^{Pso}S1 and 31 µM for ^{Mass}S1 at 20 °C and pH 7.0, as reported previously[22]. This large difference in the affinity of actin.S1 for ADP is a major characteristic of a fast vs a slow myosin isoform. As reported previously the ADP affinity for *psoas* actin.S1 was relatively unaffected by temperature (about 200 ±30 µM between 10 and 30 °C) while for

masseter the effect was much greater, with the affinity becoming weaker by ~6-fold from 9.6 µM at 10 °C to 62.4 at 30 °C, at pH 7.0.

Effect of pH: A change in pH did not affect the ADP affinity for *psoas* (Table 1) over the temperature range studied (also Figure 4C). Lowering the pH to 6.2 with ^{Mass}S1 resulted in 2-fold weaker K_{AD} values than at pH 7.0 (from 10 to 22 µM at 10 °C). However, this effect of pH was not as pronounced at higher temperatures (only weakening by 1.5 fold at 30 °C, see Table 1).

Phosphate affinity (K_{Pi})

The affinity of Pi for actin.S1 (K_{Pi}) was measured but the range of Pi concentrations accessible was restricted by the need to maintain a constant ionic strength. As P_i was increased the concentration of KCl in the buffer was decreased and the maximum phosphate concentration used was 30 mM. Figure 6 shows the plots of k_{obs} as a function of phosphate concentration for the two myosin isoforms. These show the expected inhibition as [Pi] is increased with an average K_{Pi} value of 15 mM at 10 °C decreasing to 41 mM at 40 °C for actin.^{Pso}S1 at pH 7.0. Decreasing the pH to 6.2 did not significantly affect the K_{Pi} values for ^{Pso}S1 (11 mM at 10 °C, decreasing to 32 mM at 40 °C, see also Table 1).

Repeating the measurements with ^{Mass}S1 gave a K_{Pi} of 22 mM at 10 °C, weakened to 35 mM at 20 °C (pH 7.0). Lowering the pH to 6.2 resulted in an average K_{Pi} value of 17 mM at 10 °C, weakening to 28 mM at 40 °C. Thus a differential response of slow myosin to Pi was observed with temperature, with the slow myosin while starting off less sensitive to Pi at 10°C becoming more sensitive to Pi at 40°C.

ADP affinity in the presence of phosphate (K_{ADP+Pi}) was evaluated as for the ADP affinity but using fixed amounts of inorganic phosphate (30 mM in the case of ^{Pso}S1 and 15 mM with ^{Mass}S1). The presence of 30 mM Pi weakened the ADP affinity (K_{ADP+Pi}) for actin.^{Pso}S1 3-4-fold (from about 170 µM to 890 µM at 20 °C (pH 7.0)) as shown in Figure 5A and Table 1. Repeating the measurement at different

temperatures showed the apparent K_{ADP} weakening from around 500 µM at 10-20 °C to 942 µM at 30 °C (Fig 5C and Table 1). For *masseter* the effects of Pi were less marked, with the K_{ADP} weakening only 1-2-fold across the temperature range at pH 7.0. Overall, it appears that phosphate competes with ADP binding to fast A.M, but has little effect on ADP binding in slow A.M.

Lowering the pH to 6.2 resulted in a smaller effect of phosphate on the ADP affinity for actin. ^{Pso}S1, changing only 2-fold from 228 to 514 µM at 20 °C (compared to the 3 to 4-fold change seen at pH 7.0). This reduced effect of phosphate was seen across the temperature range used. In actin. ^{Mass}S1, 15 mM Pi weakened the ADP affinity 2-fold from 47 to 94 µM at 20 °C, and a similar 2-fold weakening of the K_{ADP} in phosphate (K_{ADP+Pi}) was seen at the other temperatures used at pH 6.2.

Apparent phosphate affinity ($K_{Pi\ app}$)

The apparent affinity of phosphate for acto-myosinS1 ($K_{Pi\ app}$) in the presence of ADP was calculated from the ADP affinities measured in the absence (K_{ADP}) and presence of phosphate (K_{ADP+Pi}) as detailed in the methods. At pH 7.0 and low temperature the $K_{Pi\ app}$ of actin.^{Pso}S1 was similar to the K_{Pi} value measured (11mM and 16 mM, respectively at 10 °C). At higher temperatures the K_{Pi} of actin.^{Pso}S1 was weakened to 30-40 mM, the $K_{Pi\ app}$ however remained at about 10 mM for the whole temperature range used.

At pH 6.2 the K_{Pi} of *psoas* was 30 % tighter than at pH 7.0 but otherwise showed the same behavior as temperature was increased (weakening from 15 mM at 10 °C to 32 mM at 40 °C). The $K_{Pi\ app}$ however appears 2-fold weaker at pH 6.2 for *psoas* with 24 mM and tightens to about 16 mM as temperature is increased.

For actin.^{Mass}S1 we observed a different behavior of the apparent phosphate affinity; while the measured K_{Pi} values at pH 7.0 were similar to *psoas* across the temperature range used, the $K_{Pi\ app}$ showed distinct temperature dependence, weakening from 10 to 40 mM with temperature. The K_{Pi} values of *masseter* were unaffected by a change in pH to 6.2 and remained similar to *psoas* at 22 and 35 mM (10 and 20 °C, respectively). The $K_{Pi\ app}$ however lost its temperature dependence

when the pH was lowered to 6.2 and the value remained relatively unaffected at 10-15 mM for actin.^{Mass}S1 throughout the temperature range used.

Relevance to working muscle. Work by us and others indicated an important role for Pi in tension generation as conditions that affect actomyosin affinity affect, in proportion, force generation. With the assumption that A.M force-generating states are in an effective equilibrium with the non-force-generating states at the beginning of the working stroke, past skinned psoas fiber work suggested that, with increasing [Pi] the free energy of the states that precede Pi release decrease as −RT ln[Pi] (from the slope of the force-ln[Pi] relationship, relative to the free energy of states after Pi release, leading to progressive depopulation of the force-generating states and thus reducing tension generation (26). Earlier observations by Tesi et al (44) highlighted differences between slow and fast myofibrils in tension response to phosphate, with indications of stronger actomyosin bonds in slow muscle. The combination of low pH and high Pi was shown to synergistically inhibit velocity of contraction in skinned fibres (29, 34) adding further support to the notion that in fatigue conditions, the combined effect of Pi and protons on muscle performance would come about either by decreasing the force per bridge and/or increasing the number of low-force bridges. These and other studies indicated that the effect of Pi on its own is moderate at higher temperatures but in combination with low pH it can substantially affect muscle power by affecting actomyosin interaction. The present work adds important information to explain how Pi's interaction changes the ADP affinity for AM and ultimately ATP-induced dissociation of AM, thus the speed of the cross-bridge cycle.

Concluding remarks

The phenomena we studied are at a lower level of component configuration, solution actin and myosin S1. We cannot there account for myosin cooperativity and coordinated responses to load, which could affect the hypothesized limiting processes. While experimental data imply such cooperativities (1) emerging behaviors are difficult to assess and model, a situation further complicated by the difficulty of incorporating intra-head actions into models (31). It remains to be seen

how our findings can be intergraded at the higher level 'behavior' of large myosin ensembles interacting with actin filaments, outside or inside an organized sarcomere. It is expected that in such situations other laws may apply when the myosin type effect on contractile behavior is further modulated depending on interactions with intracellular factors and overall muscle action regulation.

We expect that, given the undisputed phenotypic effect of myosin types as observed in mammalian physiology, our data provide highly relevant insights in the mechanochemical coupling factors that distinguish the fiber types. Phosphate dependence of ATP-induced dissociation is modulated by variations in actin affinity. Such variations could help modulate the phosphate dependence of force and velocity, and may explain why phosphate sensitivity appears to be in part temperature-and muscle type-dependent.

Acknowledgements

The authors acknowledge support from various sources as follows:

MAG was supported by the British Heart Foundation grant PG30200. Also, CK, MAG research was co-financed by the European Union (European Social Fund – ESF) and Greek national funds through the Operational Program "Educational and Lifelong Learning" of the National Strategic Reference Framework (NSRF) – Research Funding Program: Thales (MuscleFun Project-MIS 377260) Investing in knowledge society through the European Social Fund.

CK thanks COST Action CM1306 'Understanding Movement and Mechanism in Molecular Machines' for relevant networking support.

References

1. **Baker JE**. Muscle force emerges from dynamic actin-myosin networks, not from independent force generators. *American journal of physiology Cell physiology* 284: C1678; author reply C1678-1679, 2003.
2. **Bloemink MJ, Adamek N, Reggiani C, and Geeves MA**. Kinetic analysis of the slow skeletal myosin MHC-1 isoform from bovine masseter muscle. *Journal of molecular biology* 373: 1184-1197, 2007.
3. **Bloemink MJ, and Geeves MA**. Shaking the myosin family tree: biochemical kinetics defines four types of myosin motor. *Seminars in cell & developmental biology* 22: 961-967, 2011.
4. **Bogdanis GC**. Effects of physical activity and inactivity on muscle fatigue. *Frontiers in physiology* 3: 142, 2012.
5. **Bogdanis GC, Nevill ME, Lakomy HK, and Boobis LH**. Power output and muscle metabolism during and following recovery from 10 and 20 s of maximal sprint exercise in humans. *Acta physiologica Scandinavica* 163: 261-272, 1998.
6. **Bottinelli R**. Functional heterogeneity of mammalian single muscle fibres: do myosin isoforms tell the whole story? *Pflugers Archiv : European journal of physiology* 443: 6-17, 2001.
7. **Cannon DT, Howe FA, Whipp BJ, Ward SA, McIntyre DJ, Ladroue C, Griffiths JR, Kemp GJ, and Rossiter HB**. Muscle metabolism and activation heterogeneity by combined 31P chemical shift and T2 imaging, and pulmonary O2 uptake during incremental knee-extensor exercise. *Journal of applied physiology* 115: 839-849, 2013.
8. **Cooke R**. Force generation in muscle. *Current opinion in cell biology* 2: 62-66, 1990.
9. **Cooke R**. Modulation of the actomyosin interaction during fatigue of skeletal muscle. *Muscle & nerve* 36: 756-777, 2007.
10. **Cooke R, Franks K, Luciani GB, and Pate E**. The inhibition of rabbit skeletal muscle contraction by hydrogen ions and phosphate. *The Journal of physiology* 395: 77-97, 1988.
11. **Coupland ME, Puchert E, and Ranatunga KW**. Temperature dependence of active tension in mammalian (rabbit psoas) muscle fibres: effect of inorganic phosphate. *The Journal of physiology* 536: 879-891, 2001.
12. **Criddle AH, Geeves MA, and Jeffries T**. The use of actin labelled with N-(1-pyrenyl)iodoacetamide to study the interaction of actin with myosin subfragments and troponin/tropomyosin. *The Biochemical journal* 232: 343-349, 1985.
13. **Crow MT, and Kushmerick MJ**. Correlated reduction of velocity of shortening and the rate of energy utilization in mouse fast-twitch muscle during a continuous tetanus. *The Journal of general physiology* 82: 703-720, 1983.
14. **Debold EP, Beck SE, and Warshaw DM**. Effect of low pH on single skeletal muscle myosin mechanics and kinetics. *American journal of physiology Cell physiology* 295: C173-179, 2008.
15. **Debold EP, Dave H, and Fitts RH**. Fiber type and temperature dependence of inorganic phosphate: implications for fatigue. *American journal of physiology Cell physiology* 287: C673-681, 2004.
16. **Debold EP, Walcott S, Woodward M, and Turner MA**. Direct observation of phosphate inhibiting the force-generating capacity of a miniensemble of Myosin molecules. *Biophysical journal* 105: 2374-2384, 2013.

17. **Egan P, Moore J, Schunn C, Cagan J, and LeDuc P**. Emergent Systems Energy Laws for Predicting Myosin Ensemble Processivity. *PLoS Computational Biology* 11: 2015.
18. **Fitts RH**. Cellular mechanisms of muscle fatigue. *Physiol Rev* 74: 49-94, 1994.
19. **Foley JM, Harkema SJ, and Meyer RA**. Decreased ATP cost of isometric contractions in ATP-depleted rat fast-twitch muscle. *The American journal of physiology* 261: C872-881, 1991.
20. **Geeves MA**. Review: The ATPase mechanism of myosin and actomyosin. *Biopolymers* 105: 483-491, 2016.
21. **Green HJ**. Mechanisms of muscle fatigue in intense exercise. *Journal of sports sciences* 15: 247-256, 1997.
22. **Hamada T, Sale DG, MacDougall JD, and Tarnopolsky MA**. Interaction of fibre type, potentiation and fatigue in human knee extensor muscles. *Acta physiologica Scandinavica* 178: 165-173, 2003.
23. **Huxley HE, and Hanson J**. The structural basis of the contraction mechanism in striated muscle. *Annals of the New York Academy of Sciences* 81: 403-408, 1959.
24. **Iorga B, Adamek N, and Geeves MA**. The slow skeletal muscle isoform of myosin shows kinetic features common to smooth and non-muscle myosins. *The Journal of biological chemistry* 282: 3559-3570, 2007.
25. **Johansen KL, Doyle J, Sakkas GK, and Kent-Braun JA**. Neural and metabolic mechanisms of excessive muscle fatigue in maintenance hemodialysis patients. *American journal of physiology Regulatory, integrative and comparative physiology* 289: R805-813, 2005.
26. **Karatzaferi C, Chinn MK, and Cooke R**. The force exerted by a muscle cross-bridge depends directly on the strength of the actomyosin bond. *Biophysical journal* 87: 2532-2544, 2004.
27. **Karatzaferi C, de Haan A, Ferguson RA, van Mechelen W, and Sargeant AJ**. Phosphocreatine and ATP content in human single muscle fibres before and after maximum dynamic exercise. *Pflugers Archiv : European journal of physiology* 442: 467-474, 2001.
28. **Karatzaferi C, de Haan A, van Mechelen W, and Sargeant AJ**. Metabolic changes in single human fibres during brief maximal exercise. *Experimental physiology* 86: 411-415, 2001.
29. **Karatzaferi C, Franks-Skiba K, and Cooke R**. Inhibition of shortening velocity of skinned skeletal muscle fibers in conditions that mimic fatigue. *Am J Physiol Regul Integr Comp Physiol* 294: R948-955, 2008.
30. **Karatzaferi C, Myburgh KH, Chinn MK, Franks-Skiba K, and Cooke R**. Effect of an ADP analog on isometric force and ATPase activity of active muscle fibers. *American journal of physiology Cell physiology* 284: C816-825, 2003.
31. **Månsson A**. Actomyosin-ADP States, Interhead Cooperativity, and the Force-Velocity Relation of Skeletal Muscle. *Biophysical journal* 98: 1237-1246, 2010.
32. **Margossian SS, and Lowey S**. Interaction of myosin subfragments with F-actin. *Biochemistry* 17: 5431-5439, 1978.
33. **Millar NC, and Geeves MA**. The limiting rate of the ATP-mediated dissociation of actin from rabbit skeletal muscle myosin subfragment 1. *FEBS letters* 160: 141-148, 1983.
34. **Nelson CR, Debold EP, and Fitts RH**. Phosphate and acidosis act synergistically to depress peak power in rat muscle fibers. *American journal of physiology Cell physiology* 307: C939-950, 2014.
35. **Nyitrai M, Rossi R, Adamek N, Pellegrino MA, Bottinelli R, and Geeves MA**. What limits the velocity of fast-skeletal muscle contraction in mammals? *Journal of molecular biology* 355: 432-442, 2006.

36. **Pate E, Bhimani M, Franks-Skiba K, and Cooke R**. Reduced effect of pH on skinned rabbit psoas muscle mechanics at high temperatures: implications for fatigue. *The Journal of physiology* 486 (Pt 3): 689-694, 1995.
37. **Pate E, and Cooke R**. Addition of phosphate to active muscle fibers probes actomyosin states within the powerstroke. *Pflugers Archiv : European journal of physiology* 414: 73-81, 1989.
38. **Reconditi M, Linari M, Lucii L, Stewart A, Sun YB, Narayanan T, Irving T, Piazzesi G, Irving M, and Lombardi V**. Structure-function relation of the myosin motor in striated muscle. *Annals of the New York Academy of Sciences* 1047: 232-247, 2005.
39. **Schiaffino S, and Reggiani C**. Fiber types in mammalian skeletal muscles. *Physiological reviews* 91: 1447-1531, 2011.
40. **Sieck GC, Fournier M, Prakash YS, and Blanco CE**. Myosin phenotype and SDH enzyme variability among motor unit fibers. *Journal of applied physiology* 80: 2179-2189, 1996.
41. **Siemankowski RF, Wiseman MO, and White HD**. ADP dissociation from actomyosin subfragment 1 is sufficiently slow to limit the unloaded shortening velocity in vertebrate muscle. *Proceedings of the National Academy of Sciences of the United States of America* 82: 658-662, 1985.
42. **Spudich JA, and Watt S**. The regulation of rabbit skeletal muscle contraction. I. Biochemical studies of the interaction of the tropomyosin-troponin complex with actin and the proteolytic fragments of myosin. *The Journal of biological chemistry* 246: 4866-4871, 1971.
43. **Tesi C, Colomo F, Nencini S, Piroddi N, and Poggesi C**. The effect of inorganic phosphate on force generation in single myofibrils from rabbit skeletal muscle. *Biophysical journal* 78: 3081-3092, 2000.
44. **Tesi C, Colomo F, Piroddi N, and Poggesi C**. Characterization of the cross-bridge force-generating step using inorganic phosphate and BDM in myofibrils from rabbit skeletal muscles. *The Journal of physiology* 541: 187-199, 2002.
45. **Walklate J, and Geeves MA**. Temperature manifold for a stopped-flow machine to allow measurements from -10 to +40 degrees C. *Analytical biochemistry* 476: 11-16, 2015.
46. **Weeds AG, and Taylor RS**. Separation of subfragment-1 isoenzymes from rabbit skeletal muscle myosin. *Nature* 257: 54-56, 1975.
47. **Westerblad H, Allen DG, and Lannergren J**. Muscle fatigue: lactic acid or inorganic phosphate the major cause? *News in physiological sciences : an international journal of physiology produced jointly by the International Union of Physiological Sciences and the American Physiological Society* 17: 17-21, 2002.
48. **Westerblad H, Bruton JD, and Lannergren J**. The effect of intracellular pH on contractile function of intact, single fibres of mouse muscle declines with increasing temperature. *The Journal of physiology* 500 (Pt 1): 193-204, 1997.

Figures & Captions

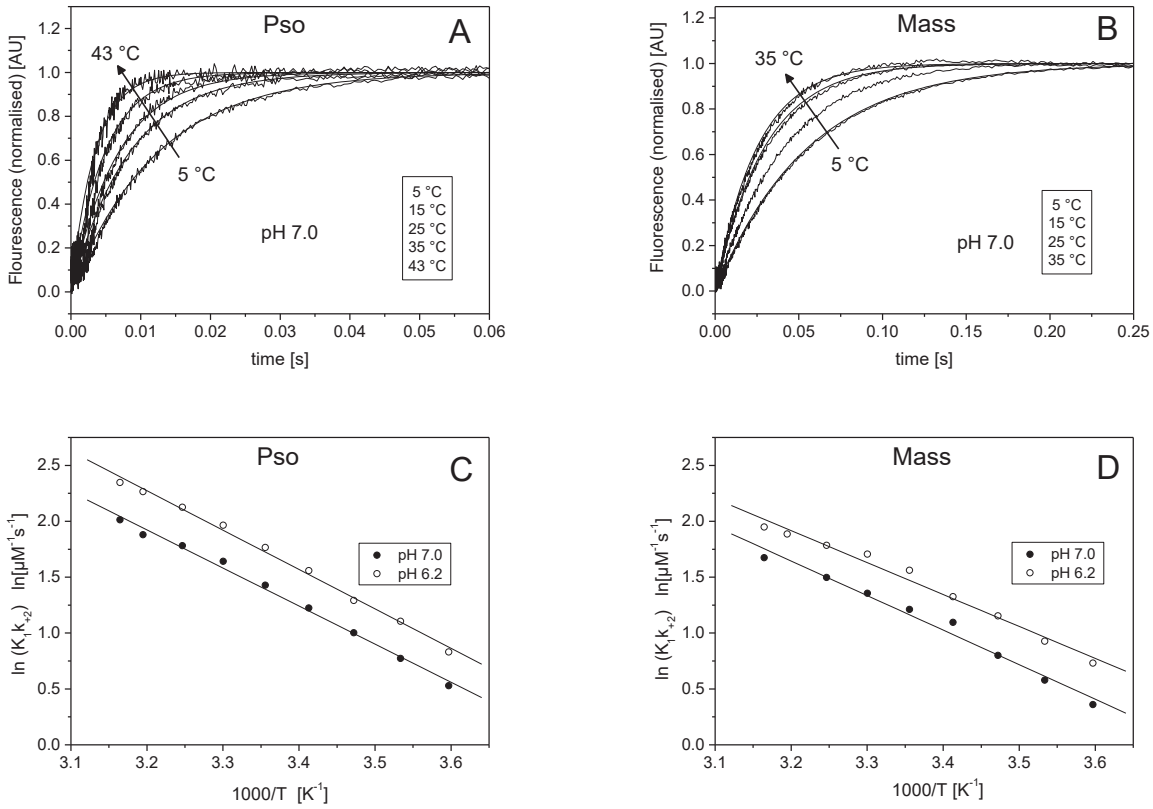

Figure 1. ATP-induced dissociation of S1 from actin, for fast (Pso) and slow (Mass) myosin isoform, at pH 7.0 and 6.2, in a range of temperatures. A. Normalized transients observed when mixing 0.5 μM pyr-act.PsoS1 with 25 μM ATP in pH 7.0 buffer at different temperatures (selected transients are shown). The change in fluorescence was fitted to a single exponential equation (best fits superimposed), giving k_{obs} of 84.8, 136.2, 208.5, 296.9, and 374.4 s^{-1} for 5, 15, 25, 35 and 43 °C, respectively. The amplitudes of the transients were relatively stable at 46 % of total fluorescence change, with some loss observed at temperatures above 30 °C. B. Normalized transients observed when mixing 0.5 μM pyrAct.MassS1 with 25 μM ATP in pH 7.0 buffer at different temperatures (selected transients are shown). The change in fluorescence was fitted to a single exponential equation (best fits superimposed), giving observed rate constants of 26.7, 36.1, 46.7, and 64.9 s^{-1} for 5, 15, 25 and 35 °C, respectively. The amplitudes of the transients were relatively stable at 40 % of total fluorescence change, with some loss observed at temperatures above 30 °C.C. Arrhenius plot of the $k_{obs}/[ATP]= K_1k_{+2}$ of Pso at pH 7.0 and pH 6.2 (temperature range 5 – 43 °C). The linear fits (best fits superimposed) gave slopes of -3.41 ±0.10 and -3.52 ±0.09 K for pH 7.0 and 6.2, respectively, from which the activation energies (Ea) were calculated as 28.3 ± 0.8 and 29.3 ± 0.8 kJ/mol. D. Arrhenius plot of the $k_{obs}/[ATP]= K_1k_{+2}$ of Mass at pH 7.0 and pH 6.2 (temperature range 5 – 43 °C). The linear fits (best fits superimposed) gave slopes of -3.09 ± 0.17 and -2.86 ± 0.14 K for pH 7.0 and 6.2, respectively, from which the activation energies (Ea) were calculated as 25.7 ± 1.4 and 23.8 ± 1.1 kJ/mol.

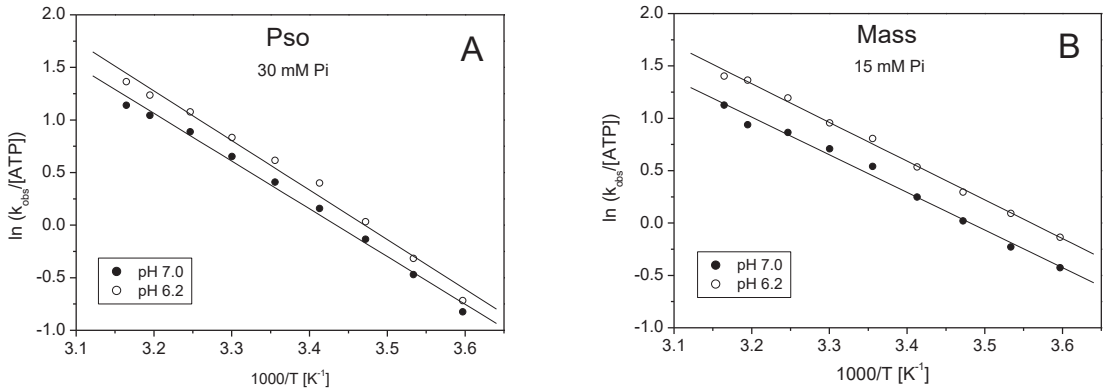

Figure 2. Effect of inorganic phosphate on the ATP-induced dissociation of S1 from actin, for fast (Pso) and slow (Mass) myosin isoform at pH 7.0 and 6.2, in a range of temperatures. A. Arrhenius plot of the k_{obs} of *Psoas* at pH 7.0 and pH 6.2 in the presence of 30 mM Pi. The linear fits (best fits superimposed) gave slopes of -4.54 ±0.15 and -4.71 ±0.20 K for pH 7.0 and 6.2, respectively, from which the activation energies (Ea) were calculated as 37.7 ± 1.2 and 39.2 ± 1.6 kJ/mol. B. Arrhenius plot of the k_{obs} of *Masseter* at pH 7.0 and pH 6.2 in the presence of 15 mM Pi. The linear fits (best fits superimposed) gave slopes of -3.59 ± 0.13 and -3.694 ± 0.08 K for pH 7.0 and 6.2, respectively, from which the activation energies (Ea) were calculated as 29.9 ± 1.1 and 30.7 ± 0.7 kJ/mol.

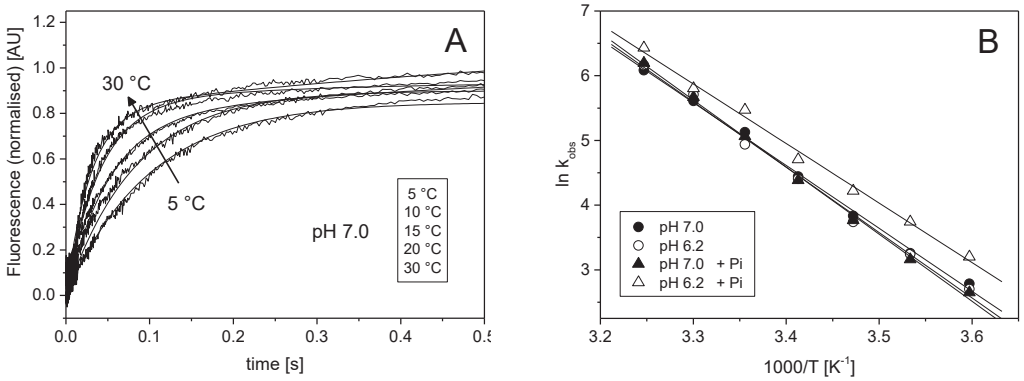

Figure 3. Temperature dependence of the ADP release from pyrAct.MassS1.A. Normalized fluorescent transients observed when 0.5 µM pyrAct.MassS1 pre-incubated with 75 µM ADP was mixed with 8 mM ATP at different temperatures between 5 and 30 °C in pH 7.0 buffer (selected transients are shown). The change in fluorescence was biphasic when observed over a time scale of 5 sec, however here only the initial fast phase is shown (fits superimposed). The k_{obs} for the fast phase were 16.2, 26.0, 46.3, 85.0 and 273 s^{-1} for 5, 10, 15, 20 and 30 °C, respectively. B. Arrhenius plot of the k_{obs} of the ADP release rate constant of *Masseter* at pH 7.0 and pH 6.2 in the absence and presence of 15 mM Pi. The linear fits (best fits superimposed) gave slopes of -9.72 ± 0.24 and -10.09 ± 0.33 K for pH 7.0 and 6.2, and -10.36 ± 0.23 and -9.20 ± 0.31 K for pH 7.0+Pi and pH 6.2 +Pi, respectively. The activation energies (Ea) were calculated as 75.9 ± 4.1 and 84.7 ± 6.1 kJ/mol for pH 7.0 and 6.2 without phosphate, and 94.4 ± 5.0 and 88.9 ± 3.9 kJ/mol for pH 7.0 and pH 6.2 respectively in the presences of phosphate.

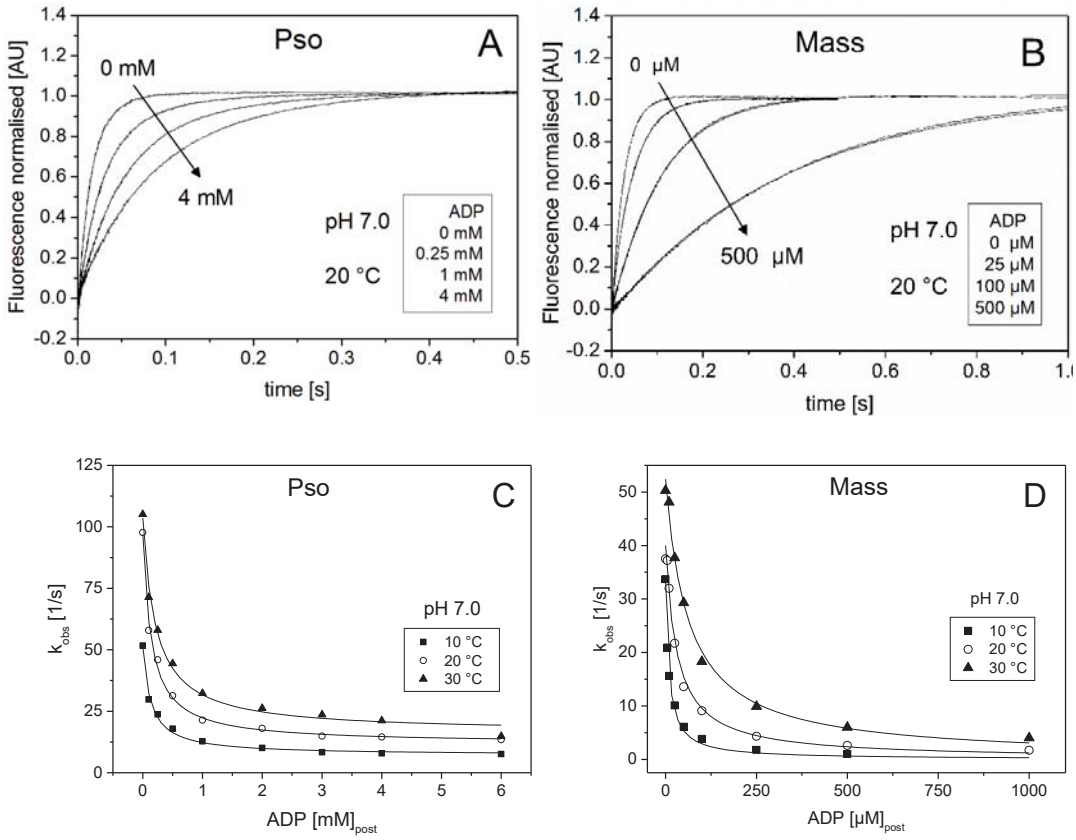

Figure 4. Temperature dependence of the ADP affinity (K_{AD}) for fast (Pso) and slow (Mass) A.S1 at pH 7.0. A. Normalized fluorescent transients observed when 0.5 µM pyrAct.PsoS1 was mixed with 25 µM ATP with various concentrations of ADP present at 20 °C in pH 7.0 buffer. The change in fluorescence was fitted by a single exponential equation (best fits superimposed). The k_{obs} determined were 87.7, 45.9, 21.4 and 14.5 s^{-1} for zero, 0.25, 1 and 4 mM ADP, respectively, with an amplitude of 30 % of total fluorescence. B. Fluorescent transients observed when 0.5 µM pyrAct.MassS1 was mixed with 25 µM ATP with various concentrations of ADP present at 20 °C in pH 7.0 buffer. The change in fluorescence was fitted to a single exponential equation (best fits superimposed). The k_{obs} determined were 37.5, 21.7, 9.1 and 2.6 s^{-1} for zero, 25, 100 and 500 µM ADP, respectively, with an amplitude of 30 % of total fluorescence. C. Plot of the observed rate constants as a function of [ADP] for *Psoas* in pH 7.0 buffer at 10, 20 and 30 °C. The data sets were fitted to a hyperbole to obtain the ADP affinity (K_{AD}) for each temperature: 131 ± 16 µM (10 °C), 140 ± 14 µM (20 °C) and 213 ± 29 µM (30 °C) for the depicted data. Refer to Table 1 for average values for from measurements in different days. D. Plot of the observed rate constants as a function of [ADP] for *Masseter* in pH 7.0 buffer at 10, 20 and 30 °C. The data sets were fitted to a hyperbole to obtain the ADP affinity (K_{AD}) for each temperature: 9.6 ± 0.7 µM (10 °C), 31.3 ± 4.0 µM (20 °C) and 62.4 ± 6.1 µM (30 °C) for the depicted data. Refer to Table 1 for average values from measurements in different days.

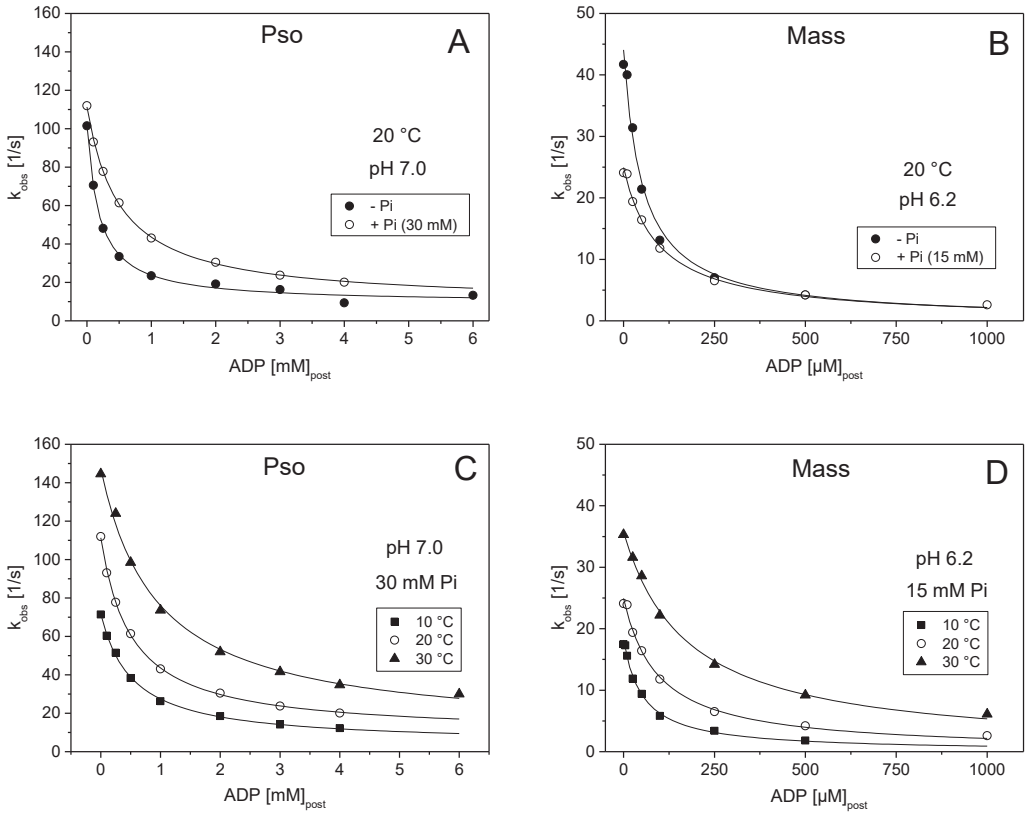

Figure 5. Effect of phosphate (Pi) on the K_{AD} of fast (Pso) and slow (Mass) A.S1. A. Plot of the observed rate constants as a function of [ADP] for *Psoas* in the presence and absence of added 30 mM Pi (pH 7.0 buffer at 20 °C). The data sets were fitted to a hyperbole to obtain the ADP affinity (K_{AD}) ± Pi: 175 ± 22 µM (no Pi) and 510 ± 22 µM (with Pi). Refer to Table 1 for average values for from measurements in different days. B. Plot of the observed rate constants as a function of [ADP] for *Masseter* in the presence and absence of added 15 mM Pi (pH 6.2 buffer at 20 °C). The data sets were fitted to a hyperbole to obtain the ADP affinity (K_{AD}) ± Pi: 48.4 ± 6.8 µM (no Pi) and 94.5 ± 8.1 µM (with Pi). Refer to Table 1 for average values for from measurements in different days. C. Plot of the observed rate constants as a function of [ADP] for *Psoas* in pH 7.0 buffer in the presence of added 30 mM Pi at 10, 20 and 30 °C. The data sets were fitted to a hyperbole to obtain the ADP affinity (K_{AD}) for each temperature: 530 ± 36 µM (10 °C), 510 ± 22 µM (20 °C) and 942 ± 117 µM (30 °C). Refer to Table 1 for average values for from measurements in different days. D. Plot of the observed rate constants as a function of [ADP] for *Masseter* in pH 6.2 buffer in the presence of added 15 mM Pi at 10, 20 and 30 °C. The data sets were fitted to a hyperbole to obtain the ADP affinity (K_{AD}) for each temperature: 52.2 ± 5.8 µM (10 °C), 94.5 ± 8.1 µM (20 °C) and 175.3 ± 9.7 µM (30 °C). Refer to Table 1 for average values for from measurements in different days.

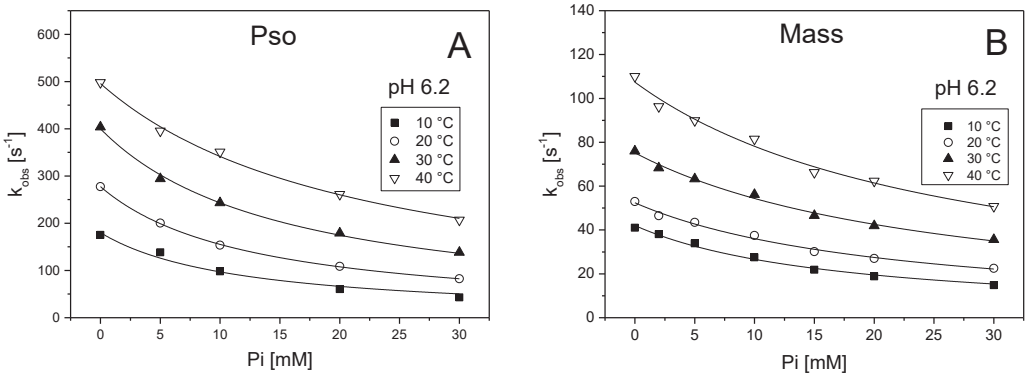

Figure 6. Phosphate (Pi) affinity for A.M in the absence of ADP (phosphate) at pH 6.2, for fast (Pso) and slow (Mass) myosin isoform. A. Plot of the observed rate constants of the ATP-induced dissociation of 0.5 µM pyrAct.S1 by 50 µM ATP as a function of [Pi] for *Psoas* (pH 6.2 buffer) at 10 to 40 °C. The data sets were fitted to a hyperbole to obtain the Pi affinity (K_{Pi}) for each temperature: 11.7 ± 1.8 mM (10 °C), 12.7 ± 0.2 mM (20 °C), 15.5 ± 0.7 mM (30 °C) and 22.1 ± 1.2 mM (40 °C). Refer to Table 1 for average values for from measurements in different days. B. Plot of the observed rate constants of the ATP-induced dissociation of 0.5 µM pyrAct.S1 by 25 µM ATP as a function of [Pi] for *Masseter* (pH 6.2 buffer) at 10 to 40 °C. The data sets were fitted to a hyperbole to obtain the Pi affinity (K_{Pi}) for each temperature: 17.3 ± 1.1 mM (10 °C), 22.0 ± 1.4 mM (20 °C), 26.1 ± 1.3 mM (30 °C) and 26.7 ± 2.1 mM (40 °C). Refer to Table 1 for average values for from measurements in different days.

Tables

Table 1. Average values of kinetic parameters describing the ATP induced dissociation rate of actin.S1 for psoas and masseter myosin, in pH 7 and 6.2, under different temperatures, in the absence or presence of added phosphate.

	Psoas S1								Masseter S1							
pH	**7.0**				**6.2**				**7.0**				**6.2**			
constant	K_{AD}	K_{AD}+ Pi *	K_{Pi}	*calc. K_{Pi}*	K_{AD}	K_{AD}+ Pi *	K_{Pi}	*calc. K_{Pi}*	K_{AD}	K_{AD}+ Pi **	K_{Pi}	*calc. K_{Pi}*	K_{AD}	K_{AD}+ Pi **	K_{Pi}	*calc. K_{Pi}*
units	µM	µM	mM	mM	µM	µM	mM	mM	µM	µM	mM	mM	µM	µM	mM	mM
10 °C	201 ±34 (n=2)	770 ±37 (n=3)	16.2 ± 1.1 (n=2)	*10.6*	256 ±32 (n=2)	665 ±39 (n=2)	11.5 ±1.1 (n=3)	*18.8*	10.3 ±1.2 (n=2)	22.5 ±2.9 (n=2)	22.3 ±4.1 (n=1)	*10.8*	21.8 ±1.3 (n=3)	52.2 ± 4.2 (n=2)	16.6 ±0.6 (n=3)	*10.8*
20 °C	203 ±13 (n=4)	919 ±72 (n=3)	28.3 ±1.8 (n=2)	*8.5*	228 ±36 (n=2)	463 ±52 (n=1)	15.6 ±1.7 (n=4)	*23.9*	29.7 ±2.8 (n=2)	44.4 ±4.6 (n=2)	35.0 ±4.4 (n=1)	*30.9*	46.8 ±3.4 (n=3)	82.6 ±5.7 (n=2)	21.3 ±0.9 (n=3)	*14.7*
30 °C	232 ± 29 (n=2)	1017 ±52 (n=3)	31.1 ±3.0 (n=2)	*8.9*	236 ±29 (n=2)	926 ±73 (n=2)	20.5 ±2.0 (n=4)	*10.3*	56.2 ±6.5 (n=2)	79.3 ±6.5 (n=2)		*40.3*	83.9 ±4.7 (n=3)	174.6 ±7.0 (n=2)	25.3 ±1.0 (n=3)	*14.2*
40 °C			41.1 ±7.8 (n=2)				31.1 ±1.6 (n=4)								27.9 ±1.7 (n=2)	

*30 mM Pi

**15 mM Pi

Table 2. Thermodynamics results (E_A values) describing the temperature dependence of the dissociation rate constant for psoas (Pso) and masseter (Mass) myosin, under pH 7 and 6.2.

		Pso		Mass	
constant	± Pi	pH 7.0	pH 6.2	pH 7.0	pH 6.2
K_1k_{+2} [kJ/mol]	-	28.3 ± 0.8	29.3 ± 0.8	25.7 ± 1.4	23.8 ± 1.1
K_1k_{+2} [kJ/mol]	+	37.7 ± 1.2	39.2 ± 1.6	29.9 ± 1.1	30.7 ± 0.7
k_{-AD} [kJ/mol]	-	N/A	N/A	75.9 ± 4.1	84.7 ± 6.1
k_{-AD} [kJ/mol]	+	N/A	N/A	94.4 ± 5.0	88.9 ± 3.9

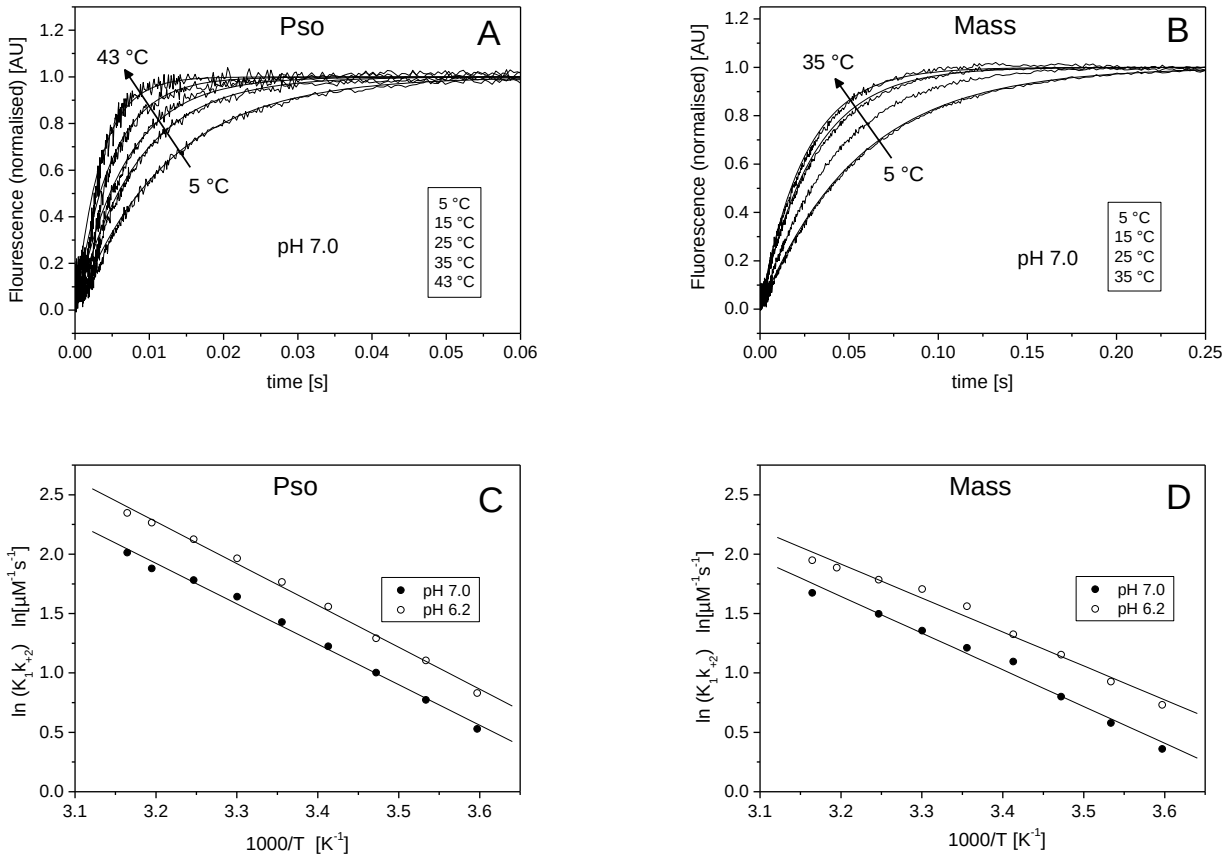

Figure 1. ATP-induced dissociation of S1 from actin, for fast (Pso) and slow (Mass) myosin isoform, at pH 7.0 and 6.2, in a range of temperatures. A. Normalized transients observed when mixing 0.5 μM pyr-act.PsoS1 with 25 μM ATP in pH 7.0 buffer at different temperatures (selected transients are shown). The change in fluorescence was fitted to a single exponential equation (best fits superimposed), giving k_{obs} of 84.8, 136.2, 208.5, 296.9, and 374.4 s^{-1} for 5, 15, 25, 35 and 43 °C, respectively. The amplitudes of the transients were relatively stable at 46 % of total fluorescence change, with some loss observed at temperatures above 30 °C. B. Normalized transients observed when mixing 0.5 μM pyrAct.MassS1 with 25 μM ATP in pH 7.0 buffer at different temperatures (selected transients are shown). The change in fluorescence was fitted to a single exponential equation (best fits superimposed), giving observed rate constants of 26.7, 36.1, 46.7, and 64.9 s^{-1} for 5, 15, 25 and 35 °C, respectively. The amplitudes of the transients were relatively stable at 40 % of total fluorescence change, with some loss observed at temperatures above 30 °C.C. Arrhenius plot of the $k_{obs}/[ATP]= K_1k_{+2}$ of Pso at pH 7.0 and pH 6.2 (temperature range 5 – 43 °C). The linear fits (best fits superimposed) gave slopes of -3.41 ±0.10 and -3.52 ±0.09 K for pH 7.0 and 6.2, respectively, from which the activation energies (Ea) were calculated as 28.3 ± 0.8 and 29.3 ± 0.8 kJ/mol. D. Arrhenius plot of the $k_{obs}/[ATP]= K_1k_{+2}$ of Mass at pH 7.0 and pH 6.2 (temperature range 5 – 43 °C). The linear fits (best fits superimposed) gave slopes of -3.09 ± 0.17 and -2.86 ± 0.14 K for pH 7.0 and 6.2, respectively, from which the activation energies (Ea) were calculated as 25.7 ± 1.4 and 23.8 ± 1.1 kJ/mol.

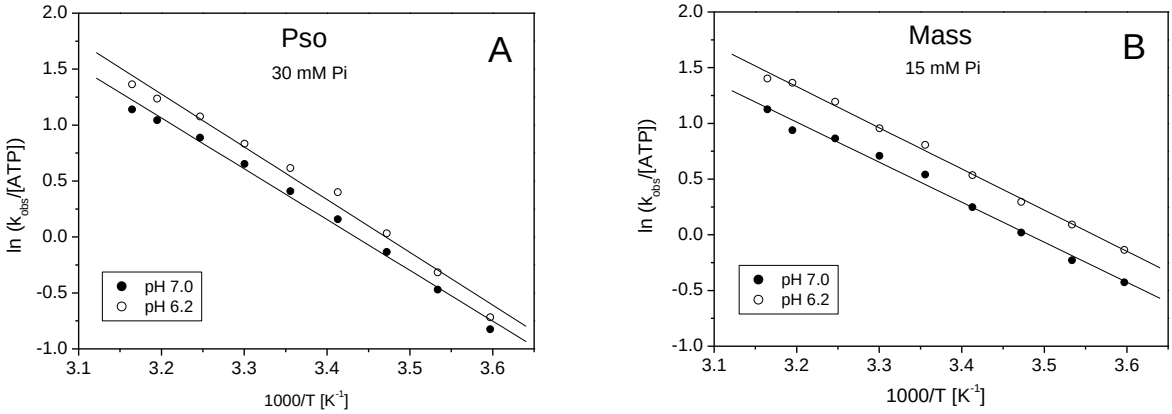

Figure 2. Effect of inorganic phosphate on the ATP-induced dissociation of S1 from actin, for fast (Pso) and slow (Mass) myosin isoform at pH 7.0 and 6.2, in a range of temperatures. A. Arrhenius plot of the k_{obs} of *Psoas* at pH 7.0 and pH 6.2 in the presence of 30 mM Pi. The linear fits (best fits superimposed) gave slopes of -4.54 ±0.15 and -4.71 ±0.20 K for pH 7.0 and 6.2, respectively, from which the activation energies (Ea) were calculated as 37.7 ± 1.2 and 39.2 ± 1.6 kJ/mol. B. Arrhenius plot of the k_{obs} of *Masseter* at pH 7.0 and pH 6.2 in the presence of 15 mM Pi. The linear fits (best fits superimposed) gave slopes of -3.59 ± 0.13 and -3.694 ± 0.08 K for pH 7.0 and 6.2, respectively, from which the activation energies (Ea) were calculated as 29.9 ± 1.1 and 30.7 ± 0.7 kJ/mol.

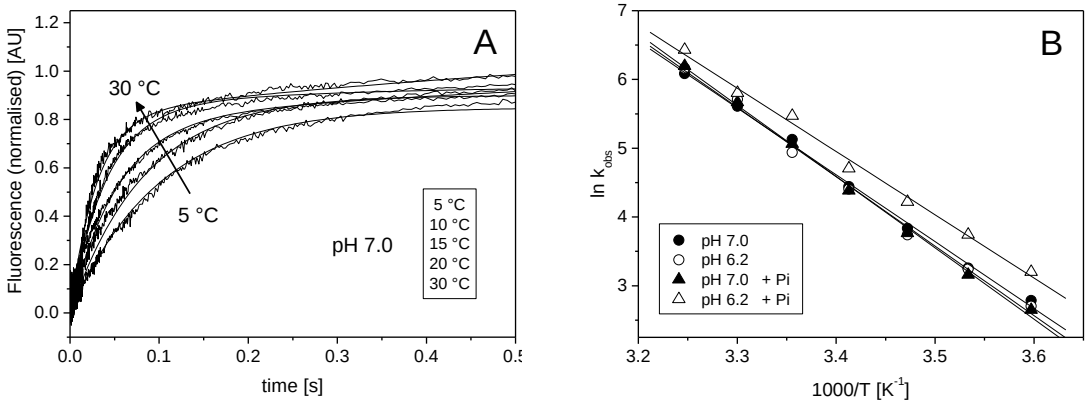

Figure 3. Temperature dependence of the ADP release from pyrAct.MassS1.A. Normalized fluorescent transients observed when 0.5 µM pyrAct.MassS1 pre-incubated with 75 µM ADP was mixed with 8 mM ATP at different temperatures between 5 and 30 °C in pH 7.0 buffer (selected transients are shown). The change in fluorescence was biphasic when observed over a time scale of 5 sec, however here only the initial fast phase is shown (fits superimposed). The k_{obs} for the fast phase were 16.2, 26.0, 46.3, 85.0 and 273 s^{-1} for 5, 10, 15, 20 and 30 °C, respectively. B. Arrhenius plot of the k_{obs} of the ADP release rate constant of *Masseter* at pH 7.0 and pH 6.2 in the absence and presence of 15 mM Pi. The linear fits (best fits superimposed) gave slopes of -9.72 ± 0.24 and -10.09 ± 0.33 K for pH 7.0 and 6.2, and -10.36 ± 0.23 and -9.20 ± 0.31 K for pH 7.0+Pi and pH 6.2 +Pi, respectively. The activation energies (Ea) were calculated as 75.9 ± 4.1 and 84.7 ± 6.1 kJ/mol for pH 7.0 and 6.2 without phosphate, and 94.4 ± 5.0 and 88.9 ± 3.9 kJ/mol for pH 7.0 and pH 6.2 respectively in the presences of phosphate.

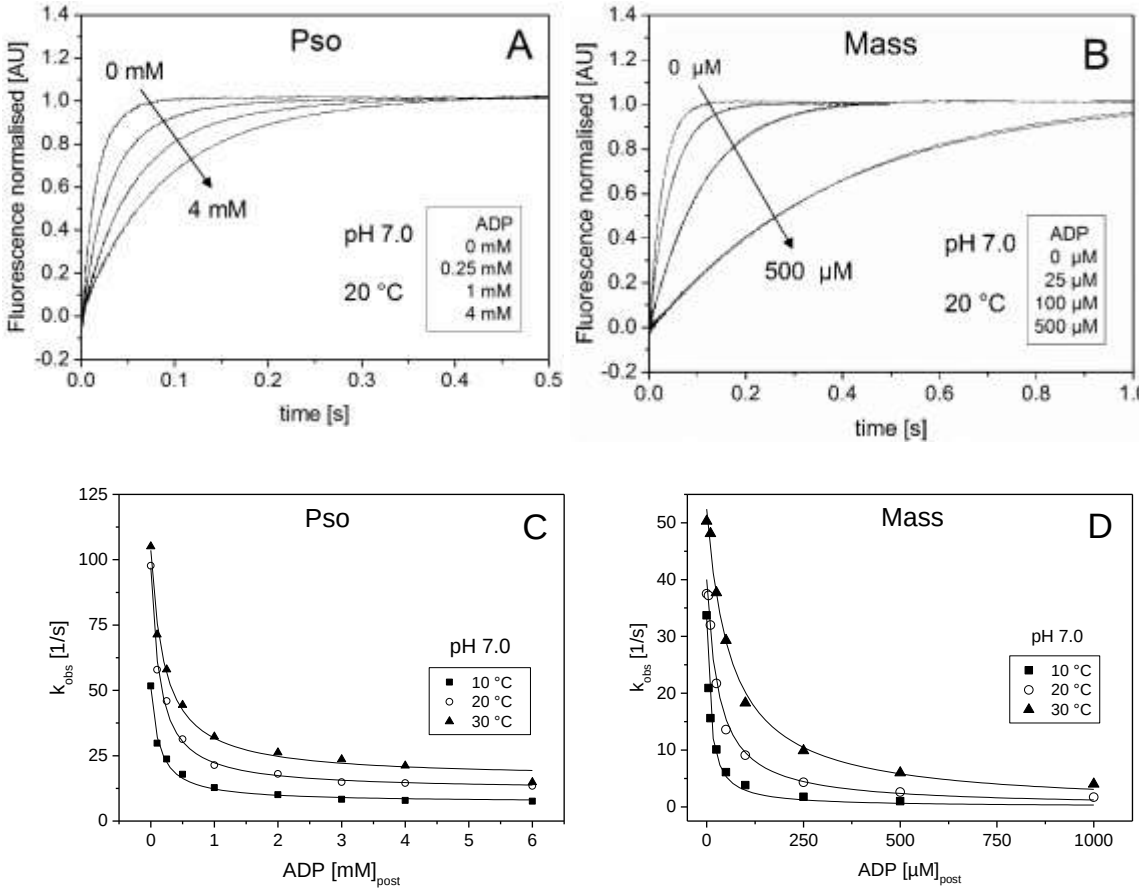

Figure 4. Temperature dependence of the ADP dissociation constant (K_{ADP}) for fast (Pso) and slow (Mass) A.S1 at pH 7.0. A. Normalized fluorescent transients observed when 0.5 µM pyrAct.PsoS1 was mixed with 25 µM ATP with various concentrations of ADP present at 20 °C in pH 7.0 buffer. The change in fluorescence was fitted by a single exponential equation (best fits superimposed). The k_{obs} determined were 87.7, 45.9, 21.4 and 14.5 s^{-1} for zero, 0.25, 1 and 4 mM ADP, respectively, with an amplitude of 30 % of total fluorescence. B. Fluorescent transients observed when 0.5 µM pyrAct.MassS1 was mixed with 25 µM ATP with various concentrations of ADP present at 20 °C in pH 7.0 buffer. The change in fluorescence was fitted to a single exponential equation (best fits superimposed). The k_{obs} determined were 37.5, 21.7, 9.1 and 2.6 s^{-1} for zero, 25, 100 and 500 µM ADP, respectively, with an amplitude of 30 % of total fluorescence. C. Plot of the observed rate constants as a function of [ADP] for *Psoas* in pH 7.0 buffer at 10, 20 and 30 °C. The data sets were fitted to a hyperbole to obtain the ADP dissociation constant (K_{ADP}) for each temperature: 131 ± 16 µM (10 °C), 140 ± 14 µM (20 °C) and 213 ± 29 µM (30 °C) for the depicted data. Refer to Table 1 for average values for from measurements in different days. D. Plot of the observed rate constants as a function of [ADP] for *Masseter* in pH 7.0 buffer at 10, 20 and 30 °C. The data sets were fitted to a hyperbole to obtain the ADP dissociation constant (K_{ADP}) for each temperature: 9.6 ± 0.7 µM (10 °C), 31.3 ± 4.0 µM (20 °C) and 62.4 ± 6.1 µM (30 °C) for the depicted data. Refer to Table 1 for average values from measurements in different days.

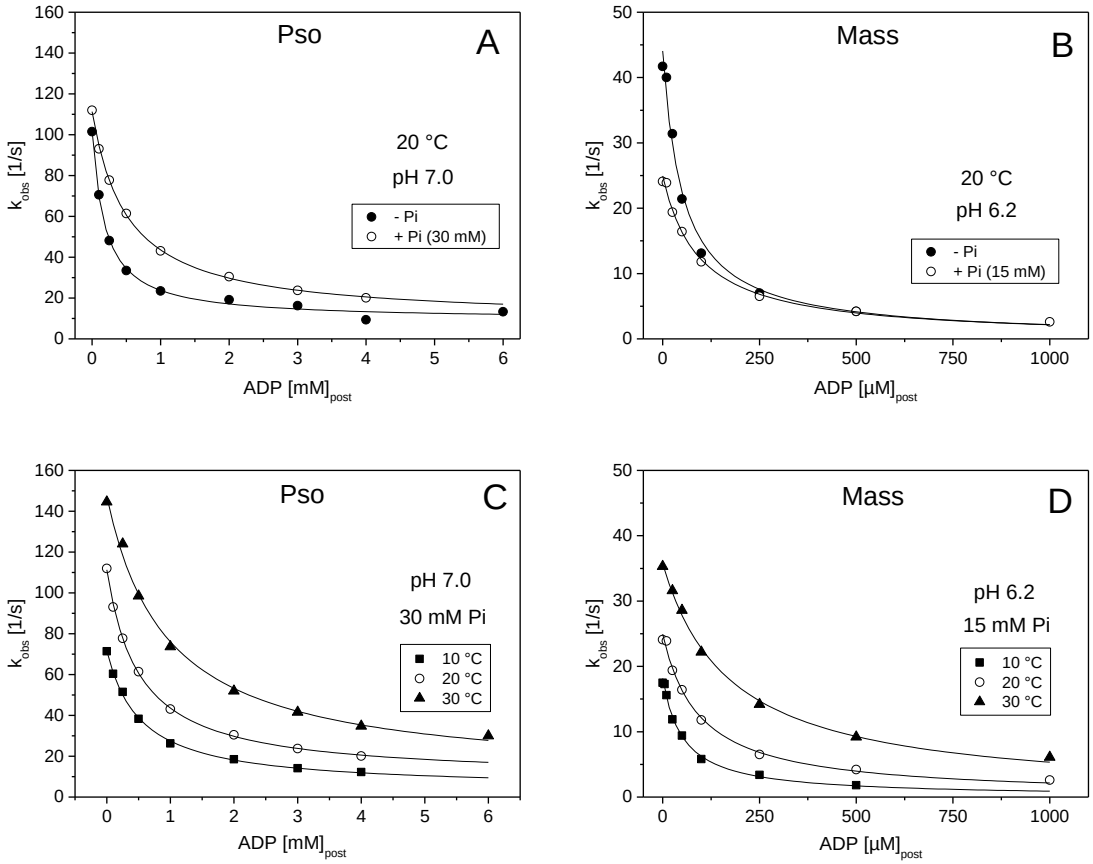

Figure 5. Effect of phosphate (Pi) on the K_{AD} of fast (Pso) and slow (Mass) A.S1. A. Plot of the observed rate constants as a function of [ADP] for *Psoas* in the presence and absence of added 30 mM Pi (pH 7.0 buffer at 20 °C). The data sets were fitted to a hyperbole to obtain the ADP dissociation constant (K_{ADP}) ± Pi: 175 ± 22 µM (no Pi) and 510 ± 22 µM (with Pi). Refer to Table 1 for average values for from measurements in different days. B. Plot of the observed rate constants as a function of [ADP] for *Masseter* in the presence and absence of added 15 mM Pi (pH 6.2 buffer at 20 °C). The data sets were fitted to a hyperbole to obtain the ADP dissociation constant (K_{ADP}) ± Pi: 48.4 ± 6.8 µM (no Pi) and 94.5 ± 8.1 µM (with Pi). Refer to Table 1 for average values for from measurements in different days. C. Plot of the observed rate constants as a function of [ADP] for *Psoas* in pH 7.0 buffer in the presence of added 30 mM Pi at 10, 20 and 30 °C. The data sets were fitted to a hyperbole to obtain the ADP dissociation constant (K_{ADP}) for each temperature: 530 ± 36 µM (10 °C), 510 ± 22 µM (20 °C) and 942 ± 117 µM (30 °C). Refer to Table 1 for average values for from measurements in different days. D. Plot of the observed rate constants as a function of [ADP] for *Masseter* in pH 6.2 buffer in the presence of added 15 mM Pi at 10, 20 and 30 °C. The data sets were fitted to a hyperbole to obtain the ADP dissociation constant (K_{ADP}) for each temperature: 52.2 ± 5.8 µM (10 °C), 94.5 ± 8.1 µM (20 °C) and 175.3 ± 9.7 µM (30 °C). Refer to Table 1 for average values for from measurements in different days.

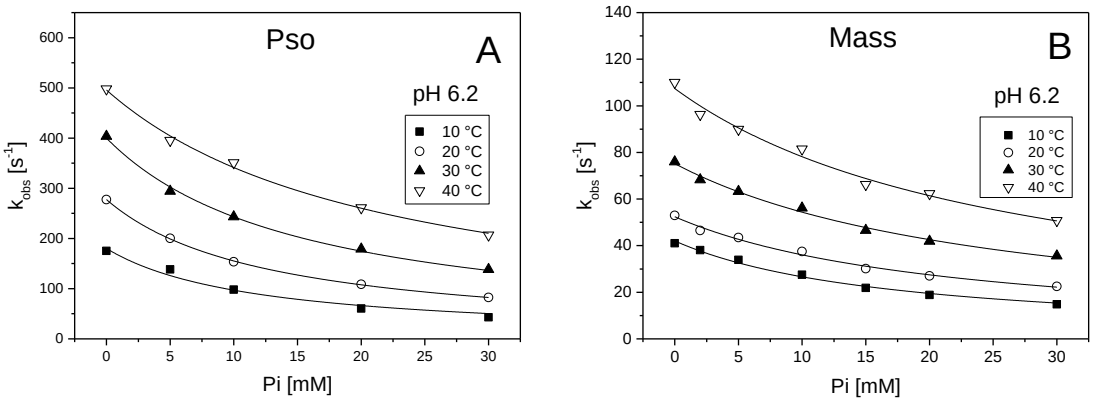

Figure 6. Phosphate (Pi) dissociation constant for A.M in the absence of ADP (phosphate) at pH 6.2, for fast (Pso) and slow (Mass) myosin isoform. A. Plot of the observed rate constants of the ATP-induced dissociation of 0.5 µM pyrAct.S1 by 50 µM ATP as a function of [Pi] for *Psoas* (pH 6.2 buffer) at 10 to 40 °C. The data sets were fitted to a hyperbole to obtain the Pi dissociation constant (K_{Pi}) for each temperature: 11.7 ± 1.8 mM (10 °C), 12.7 ± 0.2 mM (20 °C), 15.5 ± 0.7 mM (30 °C) and 22.1 ± 1.2 mM (40 °C). Refer to Table 1 for average values for from measurements in different days. B. Plot of the observed rate constants of the ATP-induced dissociation of 0.5 µM pyrAct.S1 by 25 µM ATP as a function of [Pi] for *Masseter* (pH 6.2 buffer) at 10 to 40 °C. The data sets were fitted to a hyperbole to obtain the Pi dissociation constant (K_{Pi}) for each temperature: 17.3 ± 1.1 mM (10 °C), 22.0 ± 1.4 mM (20 °C), 26.1 ± 1.3 mM (30 °C) and 26.7 ± 2.1 mM (40 °C). Refer to Table 1 for average values for from measurements in different days.

Tables

Table 1. Average values of kinetic parameters describing the ATP induced dissociation rate of actin.S1 for psoas and masseter myosin, in pH 7 and 6.2, under different temperatures, in the absence or presence of added phosphate.

	Psoas S1								**Masseter S1**							
pH	**7.0**				**6.2**				**7.0**				**6.2**			
constant	**K_{ADP}**	**K_{ADP+Pi} ***	**K_{Pi}**	***calc. K_{Pi}***	**K_{ADP}**	**K_{ADP+Pi} ***	**K_{Pi}**	***calc. K_{Pi}***	**K_{ADP}**	**K_{ADP+Pi} ****	**K_{Pi}**	***calc. K_{Pi}***	**K_{ADP}**	**K_{ADP+Pi} ****	**K_{Pi}**	***calc. K_{Pi}***
units	µM	µM	mM	mM	µM	µM	mM	mM	µM	µM	mM	mM	µM	µM	mM	mM
10 °C	201 ±34 (n=2)	770 ±37 (n=3)	16.2 ± 1.1 (n=2)	*10.6*	256 ±32 (n=2)	665 ±39 (n=2)	11.5 ±1.1 (n=3)	*18.8*	10.3 ±1.2 (n=2)	22.5 ±2.9 (n=2)	22.3 ±4.1 (n=1)	*10.8*	21.8 ±1.3 (n=3)	52.2 ± 4.2 (n=2)	16.6 ±0.6 (n=3)	*10.8*
20 °C	203 ±13 (n=4)	919 ±72 (n=3)	28.3 ±1.8 (n=2)	*8.5*	228 ±36 (n=2)	463 ±52 (n=1)	15.6 ±1.7 (n=4)	*23.9*	29.7 ±2.8 (n=2)	44.4 ±4.6 (n=2)	35.0 ±4.4 (n=1)	*30.9*	46.8 ±3.4 (n=3)	82.6 ±5.7 (n=2)	21.3 ±0.9 (n=3)	*14.7*
30 °C	232 ± 29 (n=2)	1017 ±52 (n=3)	31.1 ±3.0 (n=2)	*8.9*	236 ±29 (n=2)	926 ±73 (n=2)	20.5 ±2.0 (n=4)	*10.3*	56.2 ±6.5 (n=2)	79.3 ±6.5 (n=2)		*40.3*	83.9 ±4.7 (n=3)	174.6 ±7.0 (n=2)	25.3 ±1.0 (n=3)	*14.2*
40 °C			41.1 ±7.8 (n=2)				31.1 ±1.6 (n=4)								27.9 ±1.7 (n=2)	

*30 mM Pi

**15 mM Pi

Table 2. Thermodynamics results (E_A values) describing the temperature dependence of the dissociation rate constant for psoas (Pso) and masseter (Mass) myosin, under pH 7 and 6.2.

		Pso		Mass	
constant	± Pi	pH 7.0	pH 6.2	pH 7.0	pH 6.2
K_1k_{+2} [kJ/mol]	-	28.3 ± 0.8	29.3 ± 0.8	25.7 ± 1.4	23.8 ± 1.1
K_1k_{+2} [kJ/mol]	+	37.7 ± 1.2	39.2 ± 1.6	29.9 ± 1.1	30.7 ± 0.7
k_{-AD} [kJ/mol]	-	N/A	N/A	75.9 ± 4.1	84.7 ± 6.1
k_{-AD} [kJ/mol]	+	N/A	N/A	94.4 ± 5.0	88.9 ± 3.9